universität wien

MASTERARBEIT / MASTER'S THESIS

Titel der Masterarbeit / Title of the Master's Thesis

„Insights into the interaction of host-derived microRNAs and the gut microbiome“

verfasst von / submitted by

Jurgita Ozelyte BSc

angestrebter akademischer Grad / in partial fulfilment of the requirements for the degree of

Master of Science (MSc)

Wien, 2021 / Vienna, 2021

Studienkennzahl lt. Studienblatt / degree programme code as it appears on the student record sheet:	UA 066 830
Studienrichtung lt. Studienblatt / degree programme as it appears on the student record sheet:	Master in Molecular Microbiology, Microbial Ecology and Immunobiology
Betreut von / Supervisor:	Univ.-Prof. David Berry, Privatdoz. PhD

Acknowledgements

First and foremost, I would like to thank Dr. David Berry and Dr. Fatima Pereira for letting me be a part of this project. I am very grateful to Dr. Fatima Pereira for sharing her knowledge with me, for her positive attitude, guidance and sincere concern about the progress of the project. I would also like to thank all personnel at DOME for their help during my time there. Finally, I would like to thank to my family and friends for their support throughout this project.

Table of contents:

Abstract 9

1 Introduction 10

1.1 The gut microbiome 10

1.2 Factors affecting microbiome composition 11

1.3 Impact of faecal miRNAs on gut microbiota composition 12

1.4 Inflammatory bowel disease and the gut microbiota 13

1.5 Interplay between faecal miRNAs, microbiota and inflammatory bowel disease 14

1.6 Research performed during scientific practice 15

2 Materials and methods 17

2.1 Primers 17

2.2 Preparation of media 18

2.2.1 M9 mineral medium 18

2.2.2 BHI medium 18

2.2.3 Defined minimal media for *Bacteroides* sp. 18

2.3 Sample collection 18

2.4 Faecal sample incubation with miRNAs 19

2.5 Ethanol fixation 19

2.6 4, 6-diamidino-2-phenylindole (DAPI) staining 19

2.7 Fluorescence-activated cell sorting (FACS) 20

2.8 Fluorescence microscopy 20

2.9 DNA extraction from the sorted cells 20

2.10 Polymerase chain reaction for DNA extracts 21

2.11 16S rRNA gene sequencing 21

2.12 Data processing 21

2.13 Media and cultivation conditions of selected anaerobic organisms 21

2.14 Agar plate streaking 22

2.15 Colony PCR 22

2.16 DNA extraction from pure cultures 23

2.17 PCR product purification and Sanger sequencing 23

2.18 Inoculation of liquid bacterial cultures and bacterial growth 23

2.19 Total nucleic acid extraction from faecal samples 24

2.20 DNAse treatment 24
2.21 RNA purification 25
2.22 Agarose gel electophoresis 25
2.23 RNA quantification 25
2.24 Polyadenylation 25
2.25 Reverse Transcription (RT) 25
2.26 Preparation of standard solutions 26
2.27 Quantitative PCR 26
3 Results 27
3.1 Experimental part 1 - Assessment of gut microbiota's ability to uptake miR-21 and miR-1226 via confocal microscopy and FACS 27
3.2 Experimental part 2- Impact of miRNA supplementation on bacterial growth *in vitro* 45
3.3 Experimental part 3 - Comparison of miRNA abundance in faeces of healthy individuals and patients suffering from inflammatory bowel diseases 49
4 Discussion 54
5 References 57
6 Appendix 62
6.1 Zusammenfassung 62

List of Abbreviations:

RNA - ribonucleic acid

SPF - specific pathogen free

Hopx - HOP homeobox gene

E. coli - *Escherichia coli*

IBD - inflammatory bowel diseases

CD - Crohn's disease

UC - ulcerative colitis

MS - multiple sclerosis

EAE - experimental autoimmune encephalomyelitis

MUC1 - mucin 1

qPCR - quantitative polymerase chain reaction

PFA – paraformaldehyde

BHI - brain heart infusion

BMM – bacteroides minimal media

YCFA - Yeast extract, casitone and fatty acid

DAPI - 4, 6-diamidino-2-phenylindole

FACS – fluorescence activated cell sorting

PBS - phosphate buffer solution

RPM – rotations per minute

UV – ultraviolet

JMF - Joint Microbiome Facility

NC - negative controls

RD – random sorts

ASV - amplicon sequence variant

B. thetaiotaomicron - Bacteroides thetaiotaomicron

B. finegoldii - Bacteroides finegoldii

C. aerofaciens - Collinsella aerofaciens

F. prausnitzii - Feacalibacterium prausnitzii

C. catus - Coprococcus catus

R. gnavus - Ruminococcus gnavus

List of Tables

Table 1. List of specific primers and its sequences used for the quantitative PCR of miRNAs and 16S rRNAs..... 17
Table 2. Strains of bacteria selected for the pure culture supplemented with miRNAs growth experiments and the medium it was cultured in. 22
Table 3. Summary of significantly enriched ASVs acquired from differential abundance analysis for fluorescently labelled and sorted miR-1226 and miR-21 fractions 43
Table 4. Faecal samples acquired from patients with a given code, state of disease and indication of the presence of biofilm in ileum and cecum.. 50

List of Figures

Figure 1. Schematic representation of Experimental part 1. Assessment of gut microbiota's ability to uptake miR-21 and miR-1226 via confocal microscopy and FACS. 27
Figure 2. Gut microbiota cells incubated with 1.25 µM of miR-1226 (A,D,G), sequence from Arabidopsis thaliana (C,F,I) and DEPC water (B,E,H) at 2, 4, 6 hour time points (TP) and imaged through confocal microscopy. 29
Figure 3. Gut microbiota cells incubated with 1.25 µM of miR-21 (A), DEPC water (B) and scrambled miR-21 as a negative control (C) for 1 hour and imaged through confocal microscopy. 29
Figure 4. Representation of gating used for the FACS sorts of gut microbiota cells acquired from the faecal sample and incubated with miRNAs (A-H) 31
Figure 5. Alpha diversity metrics of microbiota in sorted fractions compared among individuals (A) and in each analysed individual (B-E) 34
Figure 6. Principal coordinate analysis (pCoA) (based on Bray-Curtis distance matrix) representing β-diversity among analyzed individuals. 35
Figure 7. Principal coordinate analysis (pCoA) (based on Bray-Curtis distance matrix) representing β-diversity within analysed individuals (A-D) 37
Figure 8. Relative abundance of bacteria interacting with supplemented miRNAs in FACS sorted fractions from the faeces of 4 analyzed individuals classified at the phylum level. 37
Figure 9. Relative abundance of bacteria interacting with supplemented miRNAs in FACS sorted fractions from the faeces of 4 analyzed individuals classified at the family level. 38
Figure 10. Differential abundance analysis using deseq2 for miR-21 in analyzed individuals 1-3 (A-C). .. 40
Figure 11. Differential abundance analysis using deseq2 for miR-1226 in analyzed individuals 1-4 (A-D).. 41
Figure 12. Schematic representation of Experimental part 2 - evaluation of miRNA induced effect on bacterial growth in vitro. 45
Figure 13. Growth of B. thetaiotaomicron and B. finegoldii in BMM (A,C) and BHI (B,D) with 1.25 µM of supplemented miR-1226 (green), miR-21 (purple), A. thaliana (negative control) (red) and DEPC water (blue) 46
Figure 14. Growth of C. aerofaciens in YCFA (A) and BHI (B), C. catus in BHI (C) and YCFA (D), F. prausnitzii in YCFA (E) with 1.25 µM of supplemented miR-1226 (green), miR-21 (purple), A. thaliana (negative control) (red) and DEPC water (blue). 47
Figure 15. qPCR strategy employed in experimental part 3 - (adapted from Balcells et al, 2011)..... 49
Figure 16. Overall distribution of all miRNA abundance levels investigated in healthy and IBD cohorts .. 51
Figure 17. Comparison of miRNA abundance levels between IBD patients, IBD controls and healthy cohort 52
Figure 18. Comparison of miRNA abundance levels between IBD patients with and without the biofilm forming in the gut. 52
Figure 19. Comparison of miRNA abundance levels between IBD control and IBD patients with ulcerative colitis..... 53

Abstract

The human gut harbors a complex community of microbes that constantly interact with each other and with the host. Epithelial gut cells have been previously shown to be able to regulate its inhabiting microbiome through production and secretion of micro ribonucleic acids (microRNA or miRNA), detectable in faeces. The aim of the project was to gain deeper understanding of the interactions of host-secreted (human) faecal miRNAs with the human gut microbiota. Previous studies with pure cultures indicated that bacteria could uptake miRNAs, resulting in altered growth and gene expression patterns. In this work we aimed to determine if and which of the members of the human gut microbiota can uptake synthetic miRNAs detected in faeces, such as hsa-miR-21 (miR-21) and hsa-miR-1226 (miR-1226), in the context of a complex community (aim 1). Even though a single bacterial species could not be identified, it was found that supplemented miRNAs tend to associate with different microbiota taxa in different individuals, suggesting that miRNA-microbiota interactions may be individual- or community-specific. Overall, miR-1226 tends to be up-taken and/or associate with several Ruminococcaceae genera, such as *Ruminococcu*s or *Faecalibacterium*, as well as by organisms from the genus *Bacteroides*. Different genera of the family Oscillospiraceae have been found to associate with miR-21 in some individuals, but not in others. Subsequently, it was looked into the ability of these two miRNAs to alter the growth of six particular microbial species (aim 2), which were selected based on results from aim 1. It was observed that *B finegoldii* and *B. thetaiotaomicron* cultured in a nutrient limited medium (but not in a rich medium) had its growth boosted by the supplemented miRNAs, which can be a consequence of altered gene expression induced by the miRNAs. Lastly, faecal samples from healthy individuals and from a cohort of patients affected by inflammatory bowel diseases (IBD) have been analyzed looking at the abundance levels of particular faecal miRNAs (aim 3). The major differences observed were lower abundance of miR-21, miR-30d, miR-320e in IBD patients compared to healthy cohort. Also miR-21 is less abundant in faeces of patients diagnosed with mucosal-associated biofilms, compared to individuals in whom biofilms are absent. Implemented methodology and results here obtained provide valuable insights on the interactions between faecal miRNAs and complex gut microbiota communities. This work serves as a base for additional experiments aiming to clarify the impact of miRNAs in microbiota composition and function, in health and disease.

1 Introduction

1.1 The gut microbiome

The field of medical science has been in progress for millenniums, starting from the primitive observations and advancing to highly complex approaches towards improving one's health. One of the newest approaches include studying human microbiome. Microbiome refers to all the bacteria, fungi, archaeae and algae, trillions of microorganisms living in association with the host in a defined environment on symbiotic, commensal or pathogenic terms (Berg *et al*, 2020). Understanding intricacies of microbiome interaction with the host could help identify ways in which health parameters can be altered for the host's benefit. One of the first examples indicating the feasibility of this concept was the work done by Linda R. Hegstrand and Roberta Jean Hine in 1986 studying the gut-brain axis. They have proved that wild-type and germ-free mice express differences in their hypothalamic histamine levels suggesting that microorganisms inhabiting humans can also affect specific aspects of human biology (Hegstrand and Hine, 1986). The interest in the human microbiome has been increasing for the past decades, nowadays reaching exponential growth, especially as new data emerges indicating that microorganisms in the gut can influence a variety of functions including host metabolism (Thursby and Juge, 2017), disposition to diseases, immunity (Gensollen *et al*, 2016) and others.

A strong symbiotic connection has formed between the host and its microbiome through thousands of years of co-evolution and its interplay is most prominently displayed in the gut due to high surface area (Neish, 2009). It is estimated that there are over a 1000 species of microbes in the large intestine, having over a 100 times more genes than the human host (Gill *et al*, 2006). More than 90% of healthy human gut bacterial species belong to four major phyla: Bacteroidetes, Firmicutes, Actinobacteria and Proteobacteria (Hugon *et al*, 2015). Unlike the inter-individual variability of human genome, which is only 0.1% among people (Wheeler *et al*. 2008), the microbiome have much greater variability and can differ by 80-90% among different host's habitats in different individuals (Ursell *et al*, 2012). A study analyzing human gut microbiome in monozygotic, dizygotic twins and their mothers, and comparing their microbial compositions to unrelated people has found that gut microbiome composition differs little within monozygotic and dizygotic twins, however the difference becomes significant when comparisons are made between twin pairs and unrelated people (Turnbaugh *et al*, 2009).

1.2 Factors affecting microbiome composition

Composition of gut microbial communities vary depending on its location within the intestine (i.e. lumen versus mucus layer; see below), as well as host's genotype, age, diet, usage of antibiotics and other drugs (Macfarlane & Macfarlane, 2003) and body's own produced miRNAs (Liu *et al*, 2016).

The impact of location on microbiome composition can be illustrated by the host's gastro-intestinal (GI) tract. Bacteria found within the mucus layer of large intestine mostly reside on outer part, as it provides more glycans for the microbes to consume and the inner mucous layer is kept uninhabited to maintain the barrier between microbiota and epithelium cells (Johansson *et al*, 2011). The inter-folds of the lumen are dominated by Lachnospiraceae and Ruminococcaceae, while the mucus are inhabited mostly by Bacteroidaceae, Prevotellaceae and Rikenellaceae (Donaldson *et al*, 2016). As the mucus layer distribution becomes uneven in the small intestine, mucus importance decreases enabling other factors, such as the presence of anti-microbial peptides (cathelicidins, C-type lectins, defensins) synthesized by the paneth cells to put survival pressures on the microbiota (Salzman *et al*, 2007).

Age is another factor influencing microbial composition in the host. The first differences arise depending on the mode of delivery and 3 years after birth, the infant's microbiota shows 40-60% resemblance to the diverse and stable adult's microbial composition (Yatsunenko *et al*, 2012).

In case when antibiotics are used, it may lead to diminished microbial ability to perform competitive exclusion – a phenomenon termed colonization resistance, which enables the beneficial bacteria to outcompete pathogenic organisms in the gut. This was first observed in 1962, when the authors noted that Salmonella infections occurred right after treatment with antibiotics (Bohnhoff and Miller, 1962).

High fat or low fiber diet can have a prolonged negative effect on the host. Microbiota composition in mice may seem to recover rapidly after the host returns to a balanced diet yet not to the same degree as it was before and the reduction in microbial diversity in the host may persist for months (Sonnenburg *et al*, 2016; David *et al*, 2014). Changes in prevalent microorganism species in the host's gut may lead to increased susceptibility of an individual to develop specific diseases due to altered repertoire of functions that a host is offered by its inhabiting species (Viennois *et al*, 2019).

MiRNAs have also been shown to impact the microbiome and it is discussed in greater details in section 1.3.

In summary, microbial communities prosper in the niches that most suit their nutrient, chemical, immunologic profiles. In return, they provide the host with a variety of functions, which have been selected by evolutionary pressures (Turnbaugh *et al*, 2009).

1.3 Impact of faecal miRNAs on gut microbiota composition

There is evidence that the host can also modulate the microbiome composition via the pool of miRNAs secreted into the gut lumen (Liu *et al*, 2016). MiRNAs are small and non-coding RNA molecules excreted by eukaryotic cells that can regulate gene expression in a post-transcriptional manner. MiRNAs bind to 3'untranslated regions of target mRNAs and further direct it towards degradation or translational repression in eukaryotes (Bartel, 2018). MiRNAs' regulatory capabilities in bacteria have been linked to changes in transcription, although the exact molecular mechanisms through which that occur are not fully understood (Liu *et al*, 2016; Liu *et al*, 2019; Teng *et al*, 2019). Liu *et al* (2016) investigated RNA isolated from gut luminal contents of mice and found that miRNA abundance differed in different parts of the gastro-intestinal tract – it was lower in the colon, where most of microbes reside and higher in the distal ileum where there are less bacteria. It was further found that more miRNAs can be detected in the faecal samples of germ free mice than in those of specific pathogen free (SPF) mice. On top of that, abundance of faecal miRNA in antibiotic treated SPF mice showed increase when compared to SPF mice that were not treated with antibiotics, thus basically suggesting that microbes modulate miRNA presence and abundance in the gut. Looking for the potential sources of miRNA in the gut resulted in discovery of intestinal epithelial cells as the main producers of gut miRNAs. This was elucidated after generation of mice whose intestinal epithelial cells had defective Dicer enzyme that cleaves RNA molecules producing mature miRNAs. Without its function, intestinal epithelial cells could no longer produce and secrete miRNAs, resulting in an altered bacterial abundance profile detected after 16S rRNA sequencing of V4 regions. It was observed that in absence of host-generated miRNAs, the levels of Bacteroidaceae and Helicobacteroidaceae increase while the levels of Prevotella decrease (Liu *et al*, 2016).

Several studies have already suggested a link between specific faecal miRNAs and the effect they can cause on bacteria inhabiting the host's gut. For example pure *E. coli* culture supplemented with hsa-miR-1226-5p has been shown to have greater growth rates than the cultures supplemented with a control, scrambled version of hsa-miR-1226-5p (Liu *et al*, 2016). This has been attributed to miRNA specific base pairing to bacterial nucleic acid sequences and effect on DNA or RNA level thus increasing the bacteria growth rates. *Enterobacteriaceae* species, mostly *E. coli* (Mukhopadhya, 2012), are abundantly found in

patients with inflammatory bowel disease or colorectal cancer and have been suggested to increase the severity of inflammatory responses in the host, leading to exacerbated disease states (Darfeuille-Michaud, 1998; Martin, 2004). A study in mice performed by Viennois *et al* (2019) found a strong correlation between the abundance of Enterobacteriaceae and miR-194-5p, miR-148-3p, miR-27b-3p. Another study by Liu *et al* (2019) have discovered that an increase in commensal bacteria *Akkermansia muciniphila* leads to suppressed multiple sclerosis (MS)-like symptoms in experimental autoimmune encephalomyelitis (EAE) mice model of MS. This increase is mediated by miR-30d, as mice supplemented with miR-30d show higher levels of *A. muciniphila.* Further tests have revealed that miR-30d is predicted to bind and modulate gene expression of β-galactosidases involved in mucin hydrolysis.

1.4 Inflammatory bowel disease and the gut microbiota

Most commonly known forms of inflammatory bowel diseases (IBDs) are Crohn's disease (CD) occurring in any part of the gastrointestinal tract and ulcerative colitis (UC) only affecting the large intestine (Fakhoury *et al*, 2014). IBDs are chronic inflammation in the intestines mostly prevalent in highly developed Western countries and though its causes are not clearly defined, the IBDs are believed to be evoked by immunologic, genetic, environmental factors (Fakhoury *et al*, 2014). Disrupted balance between Th_{17} and T_{reg} populations favoring the latter (Geuking *et al*, 2011) as well as genetic predisposition, where a monozygotic twin has over 50% chance of developing a CD when compared to 10% chance in dizygotic twins (Loddo and Romano, 2015) can both influence host susceptibility to IBDs. However, it is suggested that the tipping point in IBD onset is the breakdown of the immunologic tolerance to the host's microbiota (Round & Mazmanian, 2010).

Inflammatory bowel diseases are accompanied by changes in microbiota composition, however, it is not yet proved whether these changes are the source or the outcome of the inflammatory condition. It has also been noted that in most mouse models of IBD where bacteria are absent, less severe bowel inflammation is observed, proving the interconnection between the two (Gkouskou *et al*, 2014). Most commonly observed changes in the microbiota composition between healthy people and IBD patients included a decrease in Firmicutes and sometimes in Bacteroides and a relative increase of *Enterobacteriaceae species* (Khan *et al*, 2019).

1.5 Interplay between faecal miRNAs, microbiota and inflammatory bowel disease

MiRNA abundance profiles vary in different tissues, serum or faeces and on top of that, several miRs were reported to be up- or down-regulated in diseased patients as detailed below. MiR-21 is one of the most studied miRNAs involved in IBDs or colorectal cancer. MiR-21 has been observed to be overexpressed in affected individuals as well as in experimental models of IBD. This overexpression leads to, among other things, a reduced ability of a host to maintain tight junctions in gut epithelial cells, which may exacerbate colitis (Liu *et al*, 2016; Zhang *et al*, 2015). Consequently the decrease or a complete knock out of miR-21 levels lead to higher resistance to artificially induced colitis in mouse models (Shi *et al*, 2016; Johnston *et al*, 2018). Johnston and colleagues (2018) also showed that mice lacking miR-21 had a different constitution of microbiota than wild type mice leading to miR-21 deficient mice being less affected by DSS induced colitis. Co-habitation of both mice types also reduced wild type mice susceptibility to the colitis suggesting that the effect microbiota has on the host could be transferable (Johnston *et al*, 2018). Furthermore, discrepant differences in miR-21 levels in faecal samples of IBD patients compared with controls have been reported in the literature, with 2 studies reporting significant lower faecal levels (Schönauen *et al*, 2018; Ahmed *et al*, 2009), an another reporting an increase, although not significant (Verdier *et al*, 2019). Other studies investigating whether and which faecal miRs differ in abundance between IBD and healthy individuals have reported that out of the 345 detectable miRNAs, 38 and 51 miRNAs were significantly upregulated in the UC and CD subjects, respectively, and 107 and 68 miRNAs were significantly downregulated compared with the healthy subjects. In detail, the abundance of miR-1226, miR-548ab and miR-515-5p levels decrease with the increasing severity in IBD status (Ji *et al*, 2018). Other study by Verdier *et al* has reported more modest results, with UC patients displaying significantly higher levels of miR-223 and miR-1246 only in their faeces as compared to control (Verdier *et al*, 2019).

Variations levels detected for miR-21 and other miRs in faeces have encouraged attempts to utilize miRNA abundance levels as a biomarker for medical purposes, i.e. early disease detection, as it was already shown that miRNA levels correlate with severity of inflammation or cancer stage (Lan *et al*, 2015). Several studies have already investigated miRNAs detected in faeces as indicators of inflammatory bowel diseases (Rashid *et al*, 2020) or Crohn's disease (Wohnhaas *et al*, 2020). It was also observed that the abundance levels of faecal miRNAs demonstrate consistency when they are analysed multiple times in the same individual over a period of time providing this approach with more credibility (Link *et al*, 2010). A study performed by Schönauen *et al* (2018) compared faecal and serum miRNA abundance levels in IBD patients and

concluded that only faecal miRNAs reflect the state of disease and correlate with other presently used biomarkers, such as faecal calprotectin and C-reactive protein levels.

MiR-1226 has been observed to directly affect bacterial gene expression, manifesting in increased growth rates of *E. coli* cultures (Liu *et al*, 2016). Experiments with confocal microscopy showed that miR-1226 can be uptaken by the GFP expressing *E. coli* strain cell cultures proving ability of miRNAs' to enter the bacteria (Liu *et al*, 2016). MiR-1226 was also noted in another study to induce higher cell death rates thus functioning as a tumor suppressor in human carcinomas that overexpress mucin 1 (MUC1) oncoprotein (Jin *et al*, 2010).

A study by Liu *et al* (2016) found miR-1246 to be the most common miRNA in human faeces and second most common in the faeces of mice, while miR-320e was also found to be one of the most common faecal miRNAs detected in humans. On top of that, increase in miR-320e abundance levels correlated significantly with deteriorating cancer stages and also to the presence of metastasis making miR-320e a credible candidate for its utilization as a biomarker (Perez-Carbonell *et al*, 2015). However, presently it does not seem that faecal levels of miR-320e were investigated in IBD patients.

An increasing number of studies attempt to find correlations between the diseased state, the microbiota and the abundance levels of miRNA detectable in the faeces. The knowledge of this kind would allow to employ some miRNAs as biological markers - indicators of early disease stages more cheaply and in a non-invasive way (Phua *et al* 2014; Ahmed *et al*, 2009), as well as use them to modulate the composition and function of the gut microbiome.

1.6 Research performed during scientific practice

The uptake of individual miRNAs by complex microbiome communities has not been investigated in detail so far. Therefore the goal of the work was to evaluate if miRNAs can be uptaken by the bacteria in the faecal samples. Depletion dynamics of miR-21 supplemented to faecal samples and its potential uptake by human gut microbiome members has been previously examined during a two months long scientific practice. Supernatants from a fresh faecal sample supplemented with the miRNA were collected at different time points post-supplementation and the levels of miRNAs quantified using quantitative polymerase chain reaction (qPCR). Data acquired through qPCR indicated that around 80% of miR-21 supplemented to the diluted faecal sample is depleted within the first 3 hours and is completely undetectable in the supernatant within 6 hours of incubation. In comparison, evaluation of filtered faecal sample where bacteria was removed from the sample indicated that even after 8 hours of incubation the

supplemented miR-21 was still detected at around 50% of its initially added amount. This allowed to hypothesize that bacteria in the sample plays a crucial role in miRNA depletion and/or uptake, but nevertheless, miRNAs can also be degraded by extracellular nucleases that may be present in the sample, and that seem to act independently from live cells. Evaluation of the sample where faecal bacteria was fixed with 4% paraformaldehyde (PFA) showed that miRNA depletion rates were lower, taking over 6 hours for the miRNA to fall below detectable limits. This suggests that supplemented miRNAs may also be binding to the fixed cells unspecifically or forming aggregates, thus becoming undetectable. Overall, this data showed that different cell-dependent and independent processes may contribute to depletion of miRNAs from the faecal sample, but the live bacteria present in the sample do have a significant role in miRNA depletion and/or potential uptake.

In this work, it was investigated how bacteria in human faecal samples interact with added miR-21 and miR-1226, which microbiota members can uptake these miRNAs (Experimental part 1) and how that could affect growth of targeted organisms (Experimental part 2). Afterwards, a protocol to quantify levels of varied miRNAs in faecal samples was established, and the levels of 5 selected miRNAs were quantified in a cohort of healthy individuals and a cohort of patients suffering from inflammatory bowel diseases (Experimental part 3). The aim was to look into differences in the abundance of candidate miRNAs, to be further investigated.

2 Materials and methods

2.1 Primers

Primer	Primer sequence	Primer purpose
RT	5'- CAGGTCCAGTTTTTTTTTTTTTTTVN -3'	Reverse transcription of polyadenylated miRNAs to cDNA
hsa-miR-30d-5p_Fw:	5'-AGTGTAAACATCCCCGACT-3'	MiRNA quantification by qPCR
hsa-miR-30d-5p_Rev:	5'-GTCCAGTTTTTTTTTTTTTTTCTTCC-3'	MiRNA quantification by qPCR
hsa-miR-1246_Fw:	5'-CGCAGAATGGATTTTTGGAG-3'	MiRNA quantification by qPCR
hsa-miR-1246_Rev:	5'-GGTCCAGTTTTTTTTTTTTTTTCCTG-3'	MiRNA quantification by qPCR
hsa-miR-320e_Fw:	5'-GCAGAAAGCTGGGTTGAG-3'	MiRNA quantification by qPCR
hsa-miR-320e_Rev:	5'-GGTCCAGTTTTTTTTTTTTTTTCCTT-3'	MiRNA quantification by qPCR
hsa-miR-1226-5p_Fw	5'-GTGAGGGCATGCAGG-3'	MiRNA quantification by qPCR
hsa-miR-1226-5p_Rev:	5'-CCAGTTTTTTTTTTTTTTTCCCCAT-3'	MiRNA quantification by qPCR
hsa-miR-21-5p_Fw:	5'-GCAGTAGCTTATCAGACTGAT-3'	MiRNA quantification by qPCR
hsa-miR-21-5p_Rev:	5'-GGTCCAGTTTTTTTTTTTTTTTCAAC-3'	MiRNA quantification by qPCR
341_Fw:	5'-CCTACGGGNGGCWGCAG-3'	Amplification of V3-V4 bacterial 16S rRNA from DNA extract
785_Rev:	5'-GACTACHVGGGTATCTAATCC-3'	Amplification of V3-V4 bacterial 16S rRNA from DNA extract
616V:	5'-AGAGTTTGATYMTGGCTC -3'	Full 16S rRNA amplification for colony PCR
1492_Rev:	5'-GGYTACCTTGTTACGACTT -3'	Full 16S rRNA amplification for colony PCR

Table 1. List of specific primers and its sequences used for the quantitative PCR of miRNAs and 16S rRNA gene sequencing.

2.2 Preparation of media

2.2.1 M9 mineral medium

The M9 mineral medium used consisted of: M9 salt solution (33.7 mM of Na_2HPO_4, 22.0 mM of KH_2PO_4, 8.55 mM of NaCl, 9.35 mM of NH_4Cl), glucose 0.4%, 1 mM of $MgSO_4$, 0.3 mM of $CaCl_2$, 1 mg/ml of biotin, 1 mg/ml of thiamin, 16.8 mM of Hepes, 8.25 mM of L-cystein, trace elements solution 1X (13.4 mM of EDTA - pH 7.5, 3.1 mM of $FeCl_3$-$6H_2O$, 0.62 mM of $ZnCl_2$, 76 µM of $CuCl_2$-$2H_2O$, 42 µM of $CoCl_2$-$2H_2O$, 162 µM of H_3BO_3, 8.1 µM of $MnCl_2$-$4H_2O$).

2.2.2 BHI medium

BHI medium and BHI agar plates were prepared by dissolving brain heart infusion broth (37 g/L), yeast extract (5 g/L), L-cysteine (0.1%), agar (when needed) (1.5%) in MilliQ water and then autoclaving. Afterwards, the media was supplemented with heat sensitive components: Hemin (5 mg/L), $NaHCO_3$ (0.1% w/v) and Vitamin K1 (1 mg/L).

2.2.3 Defined minimal media for *Bacteroides* sp.

0.1% (w/v) of Glucose, 8.254 mM of L-cysteine (free base), 7.66 µM of Hemin solution, 737.8 nM of Vitamin B12, 27.45 µM of $FeSO_4$, 23.8 µM of $NaHCO_3$ solution (sterile), 6.6 mM of KH_2PO_4, 15.4 mM of NaCl, 98 µM of $MgCl_2$·6H2O, 177 µM of $CaCl_2$·$_2H_2O$, 4.2 µM of $CoCl_2$·$6H_2O$, 50.5 µM of $MnCl_2$·$4H_2O$, 9.3475 mM of NH_4Cl, 1.76 mM of Na_2SO_4 were mixed together and autoclaved except for the heat sensitive components - Hemin, $NaHCO_3$, vitamin B12 solution, which were sterilized through a 0.2µm syringe filters and added to the main solution afterwards.

2.3 Sample collection

Fresh faecal samples were collected from 10 healthy subjects. All participants followed an omnivore diet. Participants with antibiotic, probiotic, or prebiotic usage in the previous six months were excluded. The study was approved by, and conducted in accordance, with the University of Vienna ethics committee (Reference number 00161) and written informed consent was signed by all enrolled participants. Faecal samples for the IBD cohort have been acquired from AKH Hospital in Vienna, Austria. The study was approved by the ethics committee of the Medical University of Vienna (EK-Nr: 1617/2014, 1910/2019). There were 4 samples in control group, where people have had colonoscopies performed without a previous indication of disease. 6 patients had IBS and 2 had UC. 3

participants from IBS group also had biofilm found in both their ileum and cecum/colon.

2.4 Faecal sample incubation with miRNAs

This procedure has been performed to investigate the abilities of microbial communities present in the faecal sample to take up supplemented fluorescently labelled miRNAs in anaerobic environment (5% hydrogen, 10% carbon dioxide, 85% nitrogen). Prepared samples were afterwards subjected to analysis of the cells using fluorescently activated cell sorting or fluorescent microscopy. A freshly collected faecal sample was introduced into anaerobic tent (Coy labs, USA), diluted in M9 medium to 10 % (w/v), and a series of dilutions have been made to acquire final dilution of 1:25 (v/v). Particles in the tube were allowed to settle down for at least 10 minutes, and only bacteria in suspension were used for the incubations. Once ready, 1.5 – 2 ml of the diluted faecal sample was distributed into eppendorf tubes. Samples were supplemented with 1.25 µM of fluorescently labelled miR-21 or miR-1226 and respective negative controls and incubated at 37°C for 1h before harvesting the cells. After the incubation, samples were centrifuged for 6 minutes at 14 000 RPM, at room temperature and the supernatant was carefully aspirated from the tubes. The pellet was resuspended in 1 ml of PBS solution (140 mM of NaCl, 3 mM of KCl, 10 mM of Na_2HPO_4, 2 mM of KH_2PO_4 dissolved in MilliQ water, pH set to 7.4, solution autoclaved) for washing (2 times).

2.5 Ethanol fixation

Prior to analyzing the cells under the microscope, the cells have been fixed with ethanol to preserve their state. Sample was centrifuged for 6 minutes at 14 000 RPM, at room temperature followed by aspiration of the supernatant leaving only the pellet of the sample to be subjected to ethanol fixation. Pellet was resuspended in 1 volume of 100% Ethanol solution and 1 volume of 1xPBS, mixed well and incubated on ice for 20 min. Samples were then centrifuged again for 6 minutes at 14 000 RPM, at room temperature, supernatant was carefully removed and remaining pellets were subjected to DAPI staining.

2.6 4, 6-diamidino-2-phenylindole (DAPI) staining

DAPI stain attachment to the nucleic acids allows to visualize them through the confocal microscopy or FACS (fluorescence activated cell sorting) thus enabling the observer to draw conclusions about the presence of microbial organism in the analysed samples. The pellet of each sample was resuspended in 20 µl of 10 µg/µL DAPI in phosphate buffer solution (PBS) and incubated at room temperature for 15

minutes protected from light. Samples were then centrifuged for 6 minutes at 14 000 RPM, room temperature and supernatant was aspirated. The pellets were washed in 1 ml of PBS solution and then centrifuged again. Supernatant was aspirated and the pellets were resuspended in 750 – 1000 µl of 1x PBS solution, and then analyzed by FACS.

2.7 Fluorescence-activated cell sorting (FACS)

DAPI-stained samples were filtered through a cell strainer (35 µm nylon mesh) and analyzed and sorted on purity mode using a BD FACSMelody™ Cell Sorter. Gating was adjusted to the negative control samples and PBS control sample. Gating for DAPI+ and Atto488^{+}/Cy5^{+} cells was determined based on unstained cells and on cells that have been incubated with negative control-miRs labeled with Atto488 or Cy5. Fluorescence events were monitored using a 405 nm laser (for DAPI detection), a 488 nm laser and a 527/32 nm filter (for Atto488 detection), or a 561 laser and a 697/58 nm filter (for detection of Cy5 signal).

2.8 Fluorescence microscopy

10 µl of a sample was pipetted on a well of a slide for microscopy. Sample was allowed to dry by incubating it at 37°C, for 15 minutes. Procedure was repeated by pipetting additional 10 µl of the same sample on top of previously applied sample and allowed to dry. Slide was then fully submersed once in MilliQ water and dried by applying pressurized air current. 20 µl of 10 µg/µL (DAPI) in PBS stain was carefully added on top of each well containing the samples on the microscope slide and incubated at room temperature for 10 min protected from light. Afterwards, slide was fully submersed once in MilliQ water and dried by applying pressurized air current. A few drops of CitiFluor™ anti-fading mounting solution were applied to the slide before adding the coverslip. Slide was then investigated under Confocal TCS SP8X (Leica Microsystems) microscope, using 63X objective and glycerol as an imaging medium.

2.9 DNA extraction from the sorted cells

Enzymatic lysis buffer has been used to increase the efficiency of DNA extraction procedure from the FACS-sorted cells. 1.5 ml of enzymatic lysis solution (20 mM of TRIS – HCl, pH 8.0, 2 mM of Na EDTA, 1.2% v/v of Triton X – 100) has been mixed in a sterile falcon. Before usage, the solution was irradiated by UV light for 40 minutes followed by addition of 20 mg of lysozyme for every 1 ml of enzymatic lysis buffer, mixed well. For the extraction of DNA from the sorted cells the Innuprep DNA kit was used. Samples were centrifuged for 10 min at 7500 RPM and the supernatant was discarded. The pellet was resuspended in

180 µl enzymatic lysis buffer and incubated for 60 min at 37°C with gentle shaking. The DNA was extracted using the DNeasy Blood and Tissue kit (QIAGEN), according to the manufacturers instructions. Sample was eluted by adding 25 µl of DEPC water, incubated at room temperature for 5 minutes and centrifuged at for 1 minute. Eluent was stored at -20°C until further usage.

2.10 Polymerase chain reaction for DNA extracts

PCR reaction was prepared by mixing 1x DreamTaq buffer, 0.2 mM of dNTPs, 2 mM of MgCl2, 1 mM of forward (341F) and reverse (785R) primers, 2mg/ml of bovine serum albumin (BSA), 1U of Dream Taq polymerase, 1 µl of template. Samples have been denatured at 95 °C for 3 minutes and subjected to 32 cycles of 95 °C for 30 seconds, 52 °C for 30 seconds, 72 °C for 1 minute. For the final annealing step samples were kept at 72°C for 10 minutes and then stored at 4°C. After PCR, the samples have been run on 1.2% agarose gel to inspect if all the samples have been amplified successfully. Once that was confirmed the samples were further processed to be sent for sequencing.

2.11 16S rRNA gene sequencing

16S rRNA sequencing is a procedure used to identify microorganisms based on highly conserved 16S rRNA genes among species. In this project variable region V4 of 16S rRNA gene has been amplified (252 bp) via Illumina seq platform using the primers 515F (5'-GTGYCAGCMGCCGCGGTAA-3') and 806R (5'-GGACTACNVGGGTWTCTAAT-3') and analyzed using R studio. Samples were sequenced at Joint Microbiome Facility (JMF).

2.12 Data processing

The acquired data has been processed using the packages vegan (2.5.6), Phyloseq (1.32.0) and DESeq2 (1.28.1), in R studio software (1.3.959).

2.13 Media and cultivation conditions of selected anaerobic organisms

Bacterial strains to be cultured in this experiment have been selected based on the data acquired from experimental part 1.

Strain	Agar medium	Liquid Medium 1	Liquid Medium 2
Bacteroides thetaiotaomicron	BHI	Bacteroides minimal medium	BHI
Bacteroides finegoldii	BHI	Bacteroides minimal medium	BHI
Collinsella aerofaciens	BHI	YCFA	BHI
Faecalibacterium prausnitzii	YCFA	YCFA	BHI
Coprococcus catus	YCFA	YCFA	BHI
Ruminococcus gnavus	YCFA	YCFA	BHI

Table 2. Strains of bacteria selected for the pure culture supplemented with miRNAs growth experiments and the medium it was cultured in.

2.14 Agar plate streaking

In order to isolate a single genetically homogenous colony for each strain, approximately 20 µl of bacteria stored in a glycerol at -80 °C acquired from in-house gut culture collection was inoculated on a BHI or YCFA agar plate. Plates were incubated in an anaerobic tent at 37°C for 48 hours.

2.15 Colony PCR

A sterile loop was used to pick a single colony from an agar plate, which was then resuspended in 50 µl of DEPC water (filtered through 0.2 µm filter) in an eppendorf tube by vortexing briefly. Tubes were placed at -80 C° for 5 minutes followed by boiling at 95 C° for 10 minutes, to enable cell lysis. Tubes were centrifuged at 13 400 RPM for 5 minutes at room temperature and supernatant was used as a DNA template. Samples for the colony PCR were prepared by mixing 1x of Taq buffer, 0.2mM of dNTP-Mix, 2mM of MgCl2, 0.2 µM of each primer – forward (616V) and reverse (1492_Rev), 0.1 µg/µl of BSA, 1.25U of Dream DNA Polymerase, 2.5 µl of DNA template. Amplification reactions were performed in a BioRad T100 Thermal Cycler. The cycler conditions set for colony PCR were as follows: 3 minutes at 95°C, then 29 cycles of 30 seconds at 95°C, 30 seconds at 52°C, 1.5 minutes at 72°C. Last step was incubation at 72°C for 10 minutes with further storage at 4°C.

2.16 DNA extraction from pure cultures

For organisms for which cell lysis and sufficient DNA for PCR amplification are difficult to attain using the method described above, an intermediate step of DNA isolation was employed. 2.0 ml of a grown culture culture was centrifuged for 5 minutes at 13 400 RPM, at room temperature. Supernatant was discarded and the remaining pellet was subjected to DNA extraction. DNA extraction was performed using innuPREP DNA Mini Kit (Analytic Jena), following the protocol outlined in innuPREP DNA Mini kit instruction for use: Isolation from cell cultures. DNA extraction was performed only on samples subjected to alternative colony PCR procedure.

2.17 PCR product purification and Sanger sequencing

Purification of PCR products was carried in accordance with the alternative protocol of purification and concentration of PCR products from PCR reactions up to 50 µl using Innuprep PCRpure kit (Analytic jena). Sample was eluted in 20 µl of nuclease free water. PCR products have been visualized on an agarose gel and if band of interest was acquired the samples have been sent for 16S rRNA sequencing. 16S rRNA sequencing was performed in order to confirm the bacterial strains. Samples were sequenced by Microsynth AG.

2.18 Inoculation of liquid bacterial cultures and bacterial growth

Selected single colonies were taken up with a loop and inoculated into a glass tube containing 5 ml of the liquid media. Tubes were incubated at 37°C overnight, under anaerobic conditions. Inoculation of bacteroides species into defined bacterial minimum media was done 6 hours prior to inoculation of all the other remaining strains to allow more time to grow. On the following day the growth was assessed using the optical density at 600 nm. New dilutions have been prepared in eppendorf tubes to have a final OD=0.05 in 1 ml of respective media. 200 µl of the diluted sample was pipetted on a Greiner F-bottom 96 well plate in triplicates for control samples and in duplicates for the test samples. Growth curves and blank measurements for each media without inoculum were obtained using a Multiskan^{TM} FC Microplate Photometer (Thermo Fisher scientific), at 37°C. Readings were taken every 30 minutes for 48-72 hours with high intensity pulsed shakings for 10 seconds immediately before the measurement.

2.19 Total nucleic acid extraction from faecal samples

Faecal samples acquired from the healthy individuals have been collected fresh and then frozen at -80°C within 2 hours of its acquisition or alternatively, samples have been stored overnight at 4°C and frozen at -80°C immediately in the morning. Faecal samples from the patients have been provided by the AKH hospital.

For extraction of total nucleic acids (TNA) from faecal samples, ∽200 mg of frozen faecal pellets have been weighed directly into Lysing Matrix E 2 ml screw-cap tubes (MP Biomedicals) containing 500 µl of centrimonium bromide (CTAB) extraction buffer (0.35 M of NaCl, 0.12 M of CTAB, 0.008 M of KH_2PO_4 (mono), 0.17 M of $K_2HPO_4 \cdot 3H_2O$). TNA were extracted using the phenol:chloroform method. 500 µl of phenol:chloroform:isoamylalcohol (25:24:1) (Carl Roth) was added and the tubes were vortexed for 10 seconds. FastPrep-24 bead beater (M.P. Biomedicals) was used to homogenize the samples by shaking them 2x at 6.5 m/s for 30 seconds with dry ice and a 5 minutes break in between shakes. Samples were then centrifuged at 14000 RPM for 10 minutes, at 4°C. The aqueous top layer was transferred to a new 1.5 ml eppendorf tube (approximately 350 µl) and mixed with the equal amount of Choloroform:Isoamylalcohol (24:1) (Carl Roth). After gentle mixing samples were centrifuged at 14000 RPM for 10 minutes, at 4°C. The top aqueous layer (approximately 270 µl) was transferred to a new 1.5 ml eppendorf tube and additionally ∽540 µl (two times the volume of top aqueous layer) of PEG/NaCl solution (1.6M NaCl; 30 (w/v) PEG 6000) was added to the samples. Tubes were left at 4°C for 1 hour to allow the precipitation of DNA/RNA. Samples were then centrifuged at 14000 RPM, 4°C, for 15 minutes. Supernatant was carefully removed and discarded, the pellet was washed in 1 ml of cold 70% molecular biology-grade Ethanol solution. Samples were centrifuged for 10 minutes at 14000 RPM, 4°C, the ethanol was carefully removed. Samples were left with open lids for 30 minutes to allow ethanol to evaporate. 50 µl of DEPC water was added to the pellets, incubated on the bench top for 5 minutes and then the pellets were re-suspended in the added water.

2.20 DNAse treatment

In cases were RNA was to be analysed, the DNA present in the samples has been subjected to enzymatic degradation to avoid the contamination of RNA samples. Reaction was prepared by mixing 43 µl of nucleic acid crude extract, 1x TURBO DNAse I buffer (Invitrogen), 0.8 U/µl RNAse Inhibitor (Invitrogen), 0.002M DTT (Invitrogen), 0.4 U/µl TURBO DNAse I (Invitrogen) (half of wanted concentration of DNAse I was added to the mixture immediately, other half after 30 minutes of incubation). Reaction was incubated in a

thermobath (Biosan TC-100C) at 37°C for 30 minutes. Afterwards, remaining DNAse I was added to each sample followed by second incubation at 37°C for 30 minutes.

2.21 RNA purification

In order to remove the potential contaminants, the RNA samples treated with DNAse I have been subjected to RNA purification using RNA Clean and Concentrator™ kit (Zymo research) following the protocol provided with the kit. All samples were purified and eluted in 15 µl of nuclease free water, stored at -80°C until further usage.

2.22 Agarose gel electophoresis

Purified RNA samples have been analysed on 1.2% (w/v) agarose gel in 1x TBE buffer (89 mM Tris (pH 7.6), 89 mM boric acid, 2 mM EDTA). 0.0015% (v/v) of GelRed™ DNA dye (Biotium) was added to the agarose solution, followed by gentle swirling to ensure homogenous distribution of the dye. 3 µl of each sample were mixed with 1.5x of DNA loading dye (Thermo Scientific) loaded on the gel and evaluated against 1 µl of 1 kb Gene ruler DNA ladder (Thermo Scientific). Gel was left to run for 60 minutes at 100 V. Bands on a gel were visualised using Gel Doc™ XR+ transilluminator (Bio-Rad).

2.23 RNA quantification

RNA samples have been quantified using Invitrogen™ Qubit™ 4 Fluorometer and Qubit™ HS RNA Assay kit (Thermo Fisher Scientific), according to the manufacturer's instructions. .

2.24 Polyadenylation

Polyadenylation was performed prior to reverse transcribing miRNAs into cDNA by mixing 1x of PolyA polymerase buffer, 0.5 mM of rATP, 1U of PolyA polymerase (New England Biolabs GmbH) and 1.5 µg of RNA. Once ready the reactions have been placed in a PCR cycler and set up to 37°C for 30 minutes followed by 95°C for 5 minutes. Afterwards the reaction have been stored at 4°C for immediate usage or at -20°C for longer period.

2.25 Reverse Transcription (RT)

A Murine Leukemia Virus (MurL) transcriptase (New England Biolabs GmbH) was used to transcribe RNA into cDNA that can be used later as a DNA template for polymerase chain reaction. In order to be able to

determine if reverse transcription has been successful two reactions for every single sample have been set up. One of the reactions contained all necessary reagents for the procedure to work, while the other one – mock sample - did not have M-MuVL Reverse transcriptase added to the reaction tube. Reactions were prepared by mixing 1x of RT buffer, 10 mM of dNTP mix, 0.5 µM of dT adaptor primer, 2 U/µL of RNAse OUT, 10 U/µL of M-MuVL Reverse transcriptase. Afterwards, they have been placed in a thermal cycler (T100, BioRad) at 55°C for 5 minutes followed by 15 minutes at 25°C, 30 minutes at 42°C and 5 minutes at 95°C. All reactions have been further diluted by adding 130 µl of nuclease free water. Aliquots of diluted samples have been stored at -20°C and used for qPCR.

2.26 Preparation of standard solutions

One reverse transcribed sample aliquot was taken from every single sample and pooled into a new tube to produce a mixture of all samples. This mixture has been further diluted 10^{-1}, 10^{-2}, 10^{-3}, 10^{-4} and 10^{-5}. Prepared mixtures have been further used as a standard solution, as described in Barcells *et al*., 2011.

2.27 Quantitative PCR

For the quantitative PCR the master mix was prepared by mixing 1x iQ SyBr Green mix (BioRad), 0.4 µM of primer forward and reverse (see Table 1), 0.4 µM of BSA, 5 µg/µl of the template and DEPC water to bring reaction volume up to 10 µl. Samples have then been placed into a Real Time PCR detection system CFX96 (BioRad) and incubated at 95°C for 5 minutes, followed by 39 cycles of 95°C for 15 seconds, 60°C for 45 seconds and a plate read. Each sample was pipetted on a plate in triplicate by mixing 2 µl of sample with 8 µl of prepared master mix. Amplification efficiency was calculated for each set of standards prepared for a plate in accordance with the formula given below.

$$Amplification\ efficiency = \left[10 - \left(\frac{1}{Slope}\right)\right] - 1$$

Equation 1. *Calculation of qPCR amplification efficiency.*

3 Results

3.1 Experimental part 1 - Assessment of gut microbiota's ability to uptake miR-21 and miR-1226 via confocal microscopy and FACS

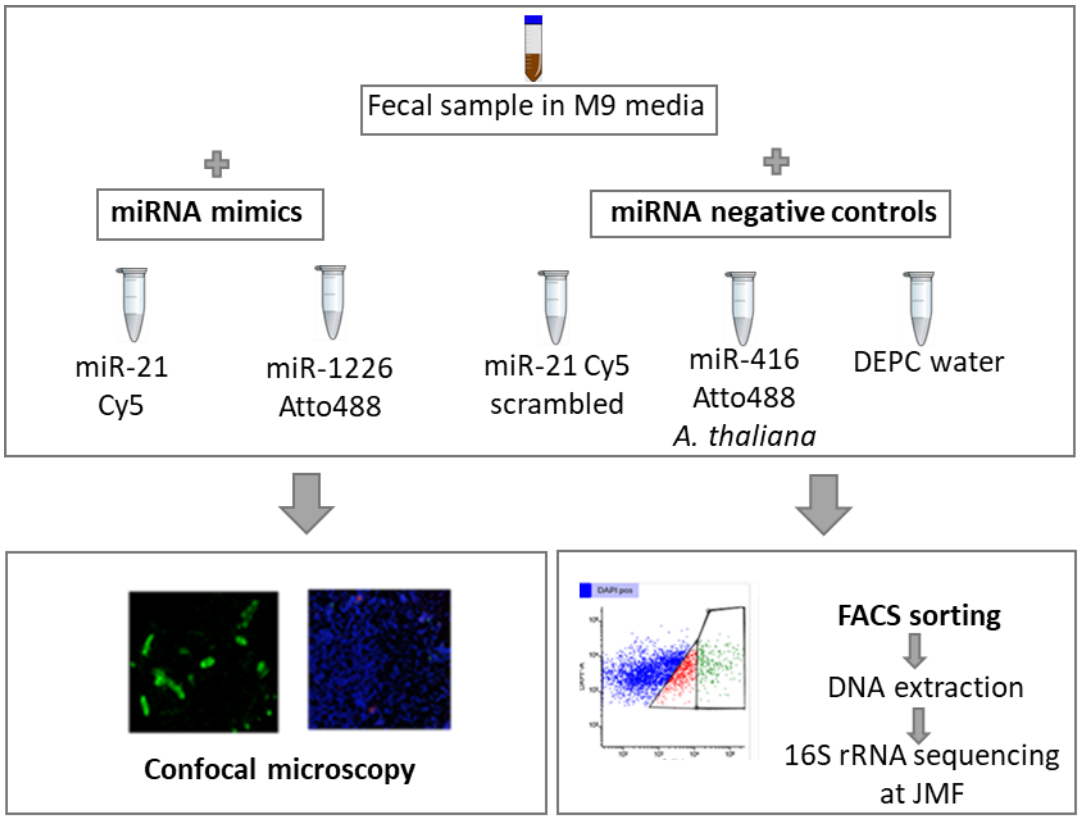

Figure 1. Schematic representation of Experimental part 1. Assessment of gut microbiota's ability to uptake miR-21 and miR-1226 via confocal microscopy and FACS.

In order to understand whether bacteria can uptake miRNAs in their environment and if miRNAs could target a specific bacterial species within the complex gut community, we started by diluting a faecal sample using M9 media (as described in the Methods section) and then supplementing it with synthetic miRs (Sigma Aldrich), which were fluorescently labeled. We tested two miRs of interest: miR-1226 was chosen because previous studies have shown that it can be uptaken by *E. coli* and increase its growth rates (Liu *et al*, 2016) therefore serving as a positive control, and miR-21 was chosen because of its implication in IBDs (Johnston *et al*, 2018). MiR-21 and its negative control (scrambled version of miR-21) were labeled with cyanine 5 (cy5) dye. Scrambled version of miRNA contains the same nucleotides, however they are rearranged to have a non-targeting stem-loop structure. MiR-1226 as well as a miRNA from the plant *Arabidopsis thaliana* (miR-416, negative control) were labelled with Atto488 dye. A sequence from *A.*

thaliana was used as a negative control of miR-1226 because it was more readily available than its scrambled version, while it is not expected to be present in the gut and also does not target human mRNAs. In a first test experiment, all prepared test samples were incubated at 37°C from 1h to 6h, fixed and analysed under confocal microscopy. Acquired images were investigated to determine if gut microbiome members could be targeted by miR-21 and miR-1226. Faecal samples incubated with 1.25 µM of fluorescently labelled miR-1226 have shown co-localization of bacteria and added miRNA molecules thus supporting the hypothesis that miRNAs may be up-taken by the bacterial cells from the gastrointestinal tract (Figure 2). The negative control miR416-Atto488 fluorescently labelled was detectable under the confocal microscope, however, it was observed to be found in the proximity of the cell but without a significant overlap with the DAPI stained cells. Fluorescently labelled miR-1226 coincides with the rod shaped bacteria that could be of the Ruminococcaceae or Lachnospiraceae families, as these families have been significantly increased in abundance in miR-1226 sorted fractions as shown in the results from differential analysis of bacterial abundance (Figure 11). Overall, fluorescence signal seemed to be maximum at earlier time points (T2 and T4).

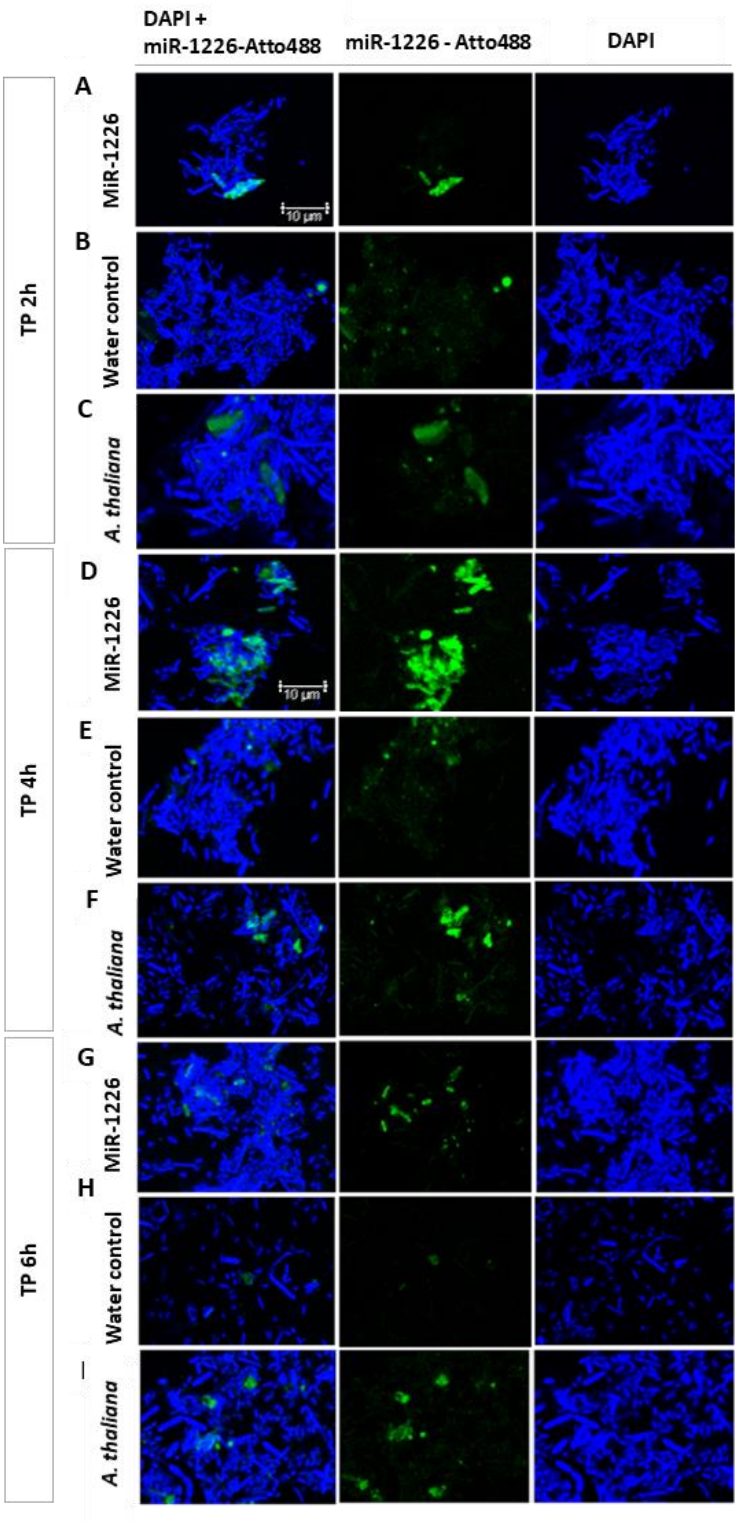

Figure 2. Gut microbiota cells incubated with 1.25 µM of miR-1226-Atto488 (A,D,G), miR-416-Atto488 (A. thaliana) (C,F,I) and DEPC water (B,E,H) at 2, 4, 6 hour time points (TP) and imaged through confocal microscopy.

Faecal samples incubated with 1.25 µM of fluorescently labelled miR-21 appear to have miRNAs localized attached to bacterial cells, but a complete co-localization with the entire cell is not observed (Figure 3).

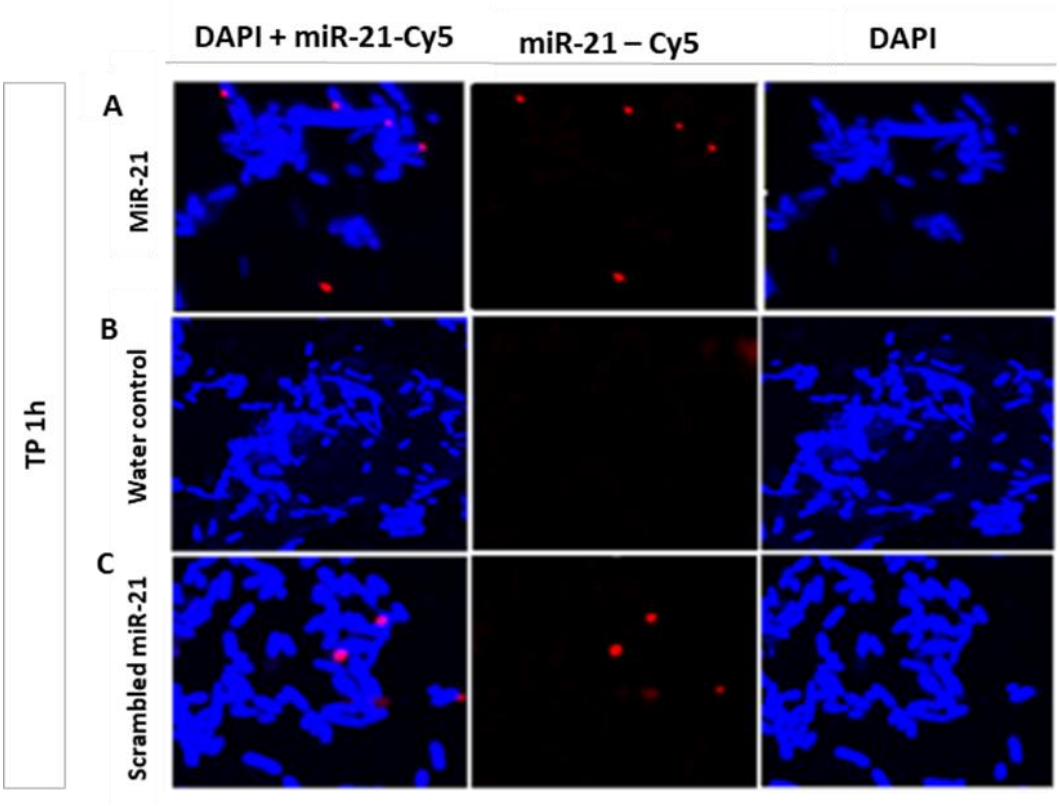

Figure 3. Gut microbiota cells cultivated with 1.25 µM of miR-21-cy5 (A), DEPC water (B) and scrambled miR-21-cy5 as a negative control (C) for 1 hour and imaged through confocal microscopy.

Faecal sample that was incubated with a negative control - scrambled miR-21 showed a similar pattern, but overall less signal than the actual sample. Nevertheless, in neither of miR-21 supplemented samples an overlap was observed between bacteria and added miRNA as in samples incubated with miR-1226. This could be due to low fluorescence of the supplemented miRNAs or fast cleavage and/or detachment of the fluorescent dye from the miR, and therefore this experiment would require to be repeated in the future studies before drawing any further conclusions. It would also be interesting in the future to do a simultaneous supplementation with both miR21-cy5 and mir-1226-Atto488 to determine whether we do see simultaneous interaction between the same individual cell with both miRs, or whether different cells uptake different miRs.

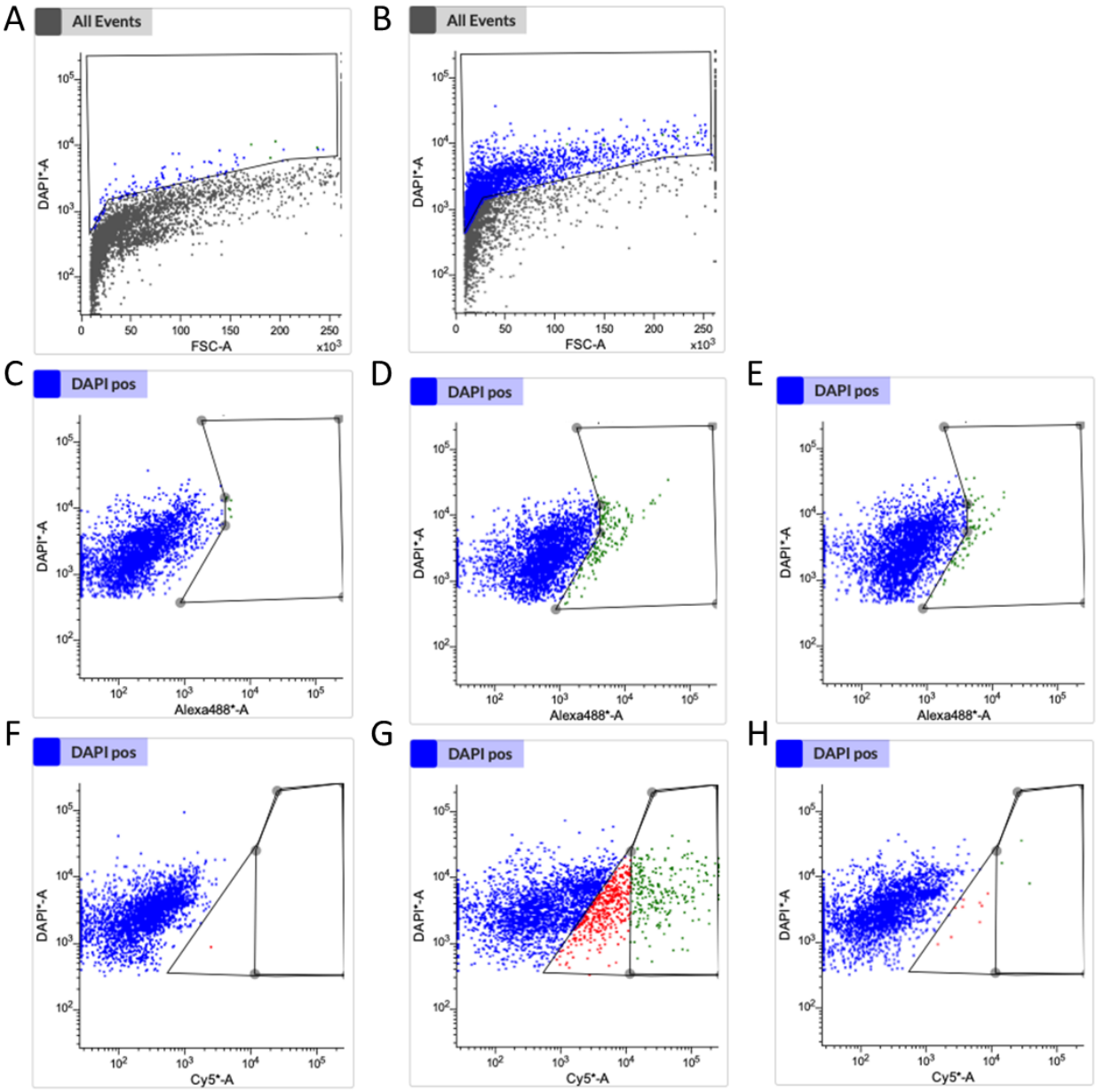

Figure 4. Representation of gating used for the FACS sorts of gut microbiota cells acquired from the faecal sample and incubated with miRNAs (A-H). DAPI negative (DAPI⁻) (A), DAPI positive (DAPI⁺) (B), PBS control (C), miR-1226-Atto488 (D), sequence from Arabidopsis thaliana-Atto488 (E), PBS control (F), miR-21-Cy5 (G), scrambled miR-21-Cy5 (H), Gating applied to F-H samples was split into two for more specificity.

For FACS sorting of faecal samples incubated in the presence of fluorescently labelled miRNAs, only DAPI positive events (DAPI$^+$; indicative of actual cells, and not noise or particles) and Atto488 or Cy5 positive events (Atto488$^+$ or cy5$^+$) were considered and sorted. DAPI$^+$ cells and gating were selected by comparing DAPI stained samples against non-DAPI stained samples. Gates to select for either Atto488$^+$ or cy5$^+$ fluorescent cells (due to miR uptake or binding) were determined based on the labeled miR negative

controls ran in parallel (Figure 4). Only events (or cells) showing higher fluorescent signals than what was recorded in the respective negative control were selected for sorting. The best time point for these analysis (1 hour of incubation) was selected after a test experiment in which 0.5, 1 and 3 hours incubation were analysed, and that showed that 1h incubations results in a higher number of fluorescent events in comparison with the negative controls. Random sorts (RD) of $DAPI^+$ cells, that would represent the overall constitution of microbiota after the entire sorting protocol, were also performed in parallel. For each sample supplemented with the miR of interest we have sorted a similar number of $DAPI^+$ cells (RD sorts) and compared the outcome (in terms of the sorted fraction taxonomic profiles) with the $DAPI^+$ $Atto488^+$/ $cy5^+$ fractions. MiR-21-cy5 sorted fractions had two gates set up for more specificity (Figure 4), however that had no effect on the end result where composition and abundance of bacteria in the sorted fractions was investigated. In total, samples acquired from 4 individuals were analysed with 2 replicates of each type, aiming at 50000 cells per sort. For a few sorted fractions the number of acquired cells was too little and amplification was not successful. All sorted fractions have been collected, its DNA was extracted, and amplified using primers targeting the v4 region of the 16S rRNA gene. None of the PBS negative control samples showed amplification, indicative of contamination during sorting and/or DNA extraction. Nevertheless, we also sequenced the PBS fractions, as a negative control.

16S rRNA sequencing of sorted fractions generated an average of 20000 reads per analysed samples. Sequencing data has been analysed with phyloseq in the R software to determine α-diversity, β-diversity, bacteria abundance levels in all analysed samples as shown in Figures 5-11.

A

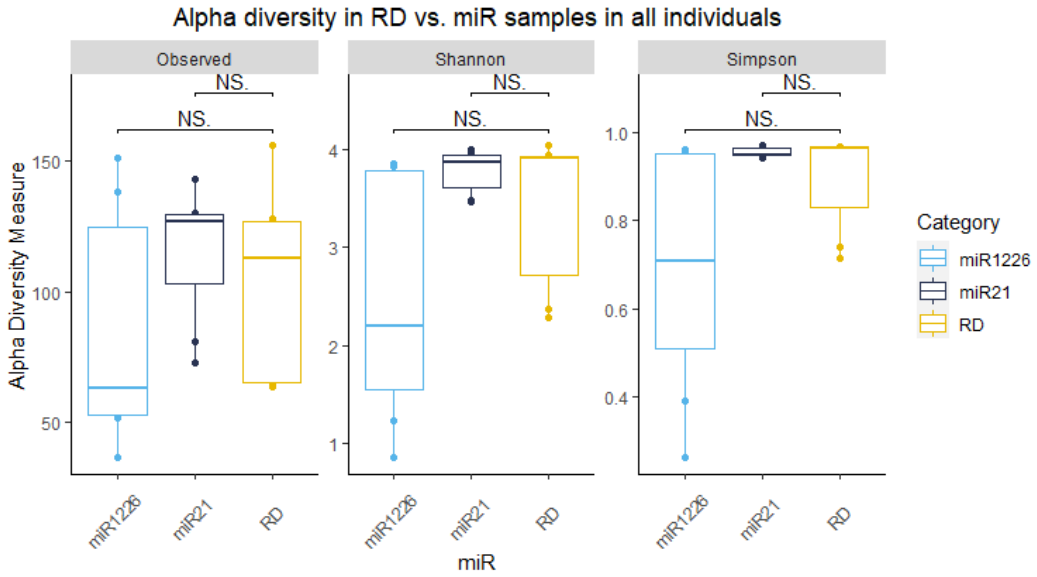

B

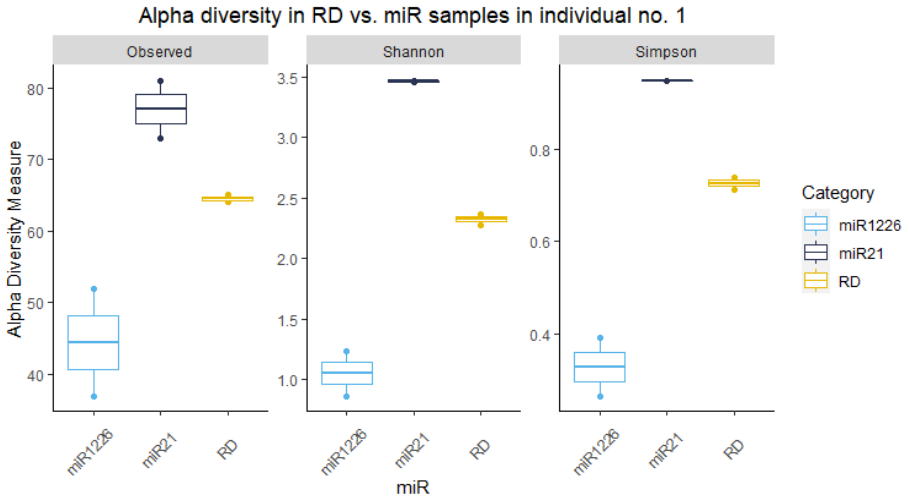
Alpha diversity in RD vs. miR samples in individual no. 1
Observed
Shannon
Simpson
Alpha Diversity Measure
miR
miR1226
miR21
RD
Category

C

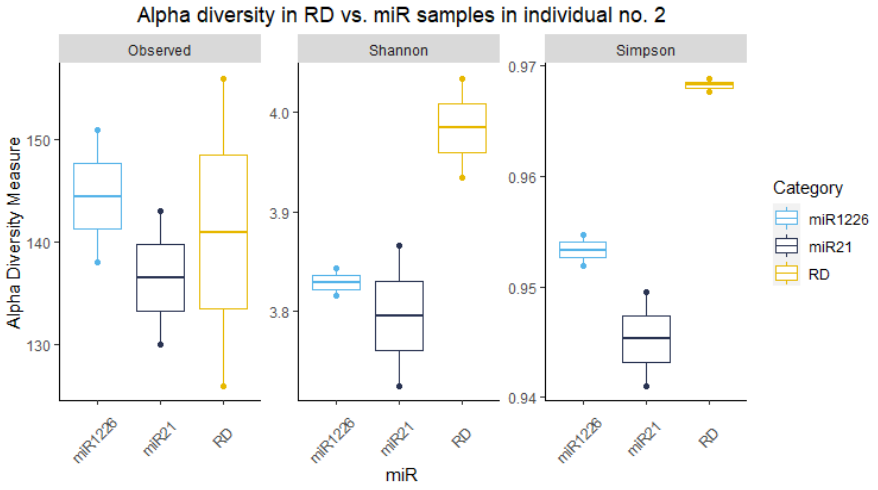
Alpha diversity in RD vs. miR samples in individual no. 2
Observed
Shannon
Simpson
Alpha Diversity Measure
miR
miR1226
miR21
RD
Category

D

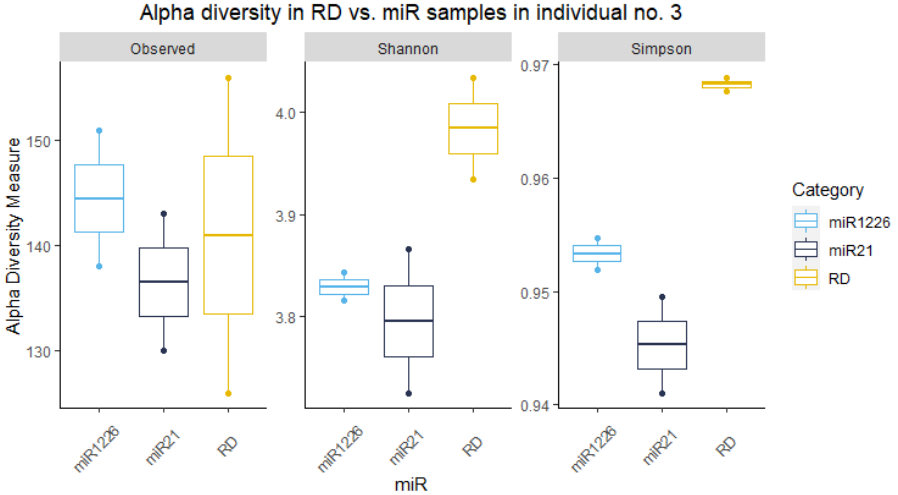
Alpha diversity in RD vs. miR samples in individual no. 3
Observed
Shannon
Simpson
Alpha Diversity Measure
miR
miR1226
miR21
RD
Category

E

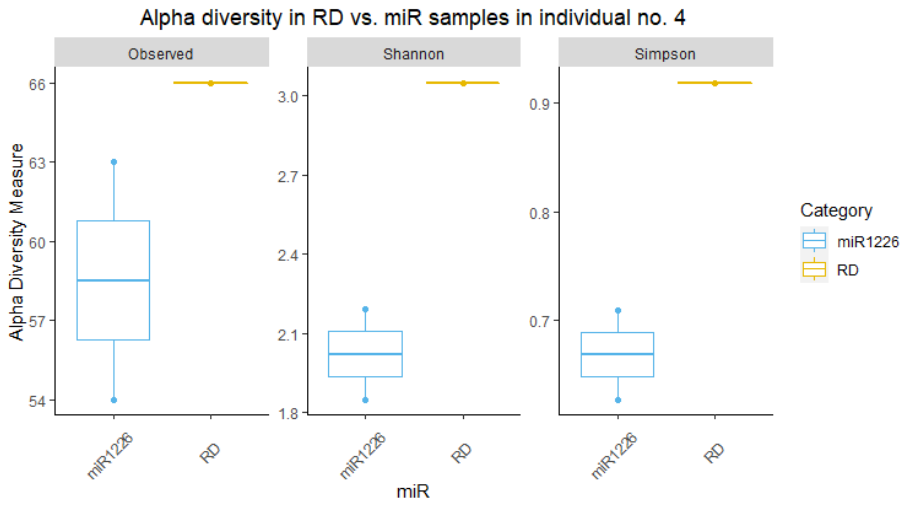

Figure 5. Alpha diversity metrics of microbiota in sorted fractions compared among individuals (A) and in each analysed individual (B-E). MiR-1226 and miR-21 samples compared against the randomly sorted fractions (RD), α-diversities displayed as Observed, Shannon and Simpson indices.

Wilcoxon test was used to calculate α-diversities in Atto488$^+$ and cy5$^+$ sorted fractions compared against the randomly sorted samples. There was no significant difference overall, although within each individual it is observed that, with the exception of individual number 2, the miR-1226-Atto488$^+$ fractions tend to have reduced diversity (Shannon and Simpson index) when compared with the RD fraction. This suggests that miR-1226 is uptaken by less diverse bacterial communities than miR-21. However the number of samples collected per miR and per individual is low and more data would be necessary to draw stronger conclusions. Data in Figure 5 also shows that there may be more than a single bacterial species that uptake the supplemented miRNA.

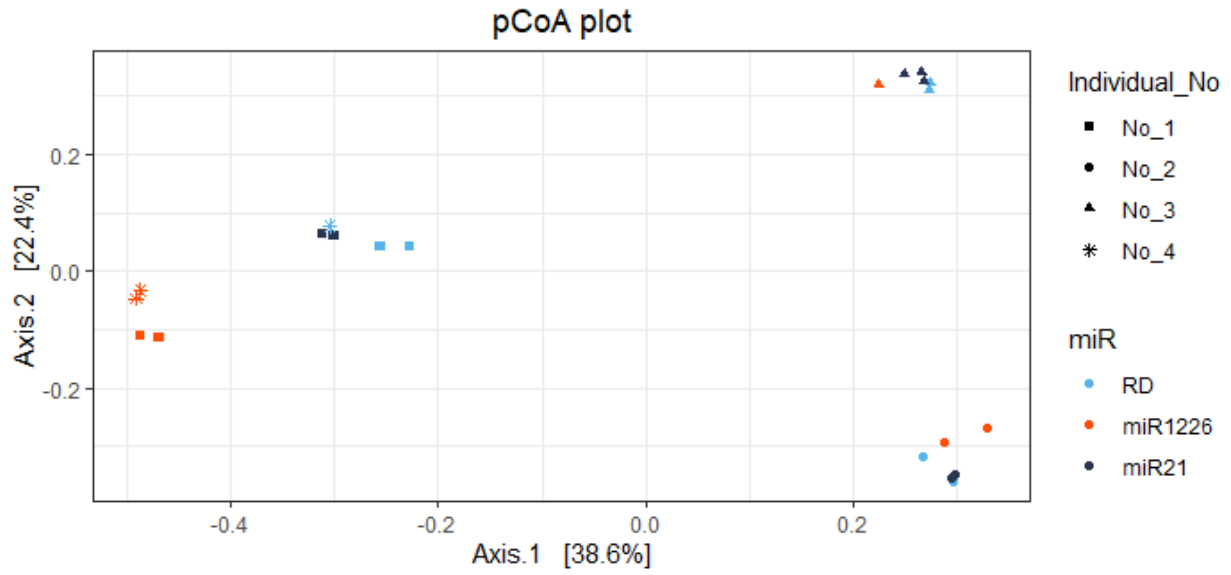

Figure 6. Principal coordinate analysis (pCoA) (based on Bray-Curtis distance matrix) representing β-diversity among analyzed individuals. Individual number is represented by shape and sample type is represented by color.

β-diversity analysis was performed to assess how much variation there is when comparing specific miR uptaking communities in different individuals. Principal coordinate analysis plot (pCoA) (Figure 6) of all samples and all analyzed individuals indicated that gut communities (in terms of the profile and abundance of total ASVs in the analysis) tend to cluster together based on the individual rather than on the sample type. It is best seen in clusters from individual No. 3 and No. 2 (Figure 6). An overlap of the communities seen in individual No. 1 and No. 4 be driven by co-habitation. In comparison, Figure 7 shows β-diversity within each analysed individual. Clusters of several same color data points indicate a degree of consistency in results from sorted sample replicates and a spatial separation indicates differentiation in the gut communities uptaking specific supplemented miRNAs.

A

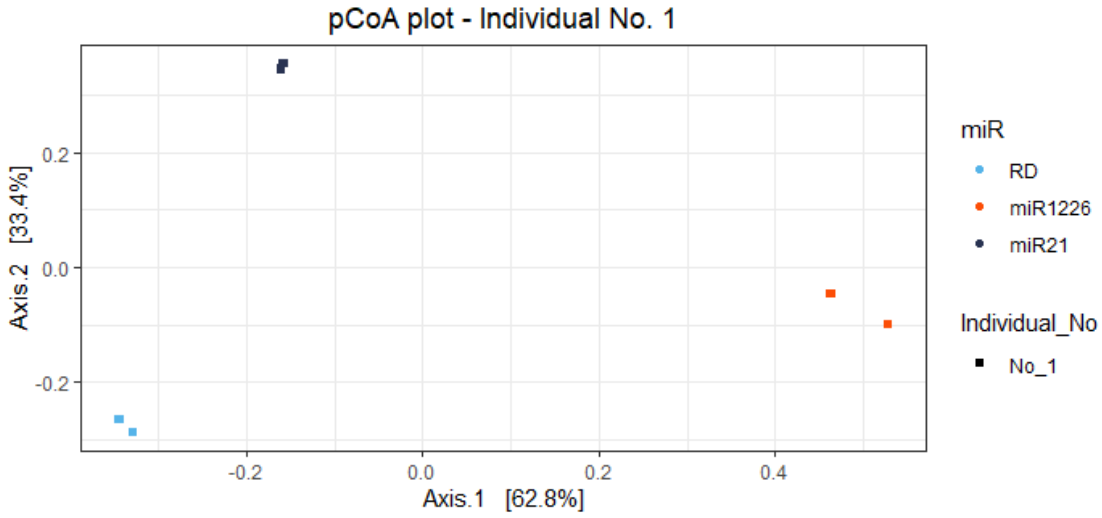
pCoA plot - Individual No. 1
Axis.2 [33.4%]
Axis.1 [62.8%]
0.2
0.0
-0.2
-0.2
0.0
0.2
0.4
miR
RD
miR1226
miR21
Individual_No
No_1

B

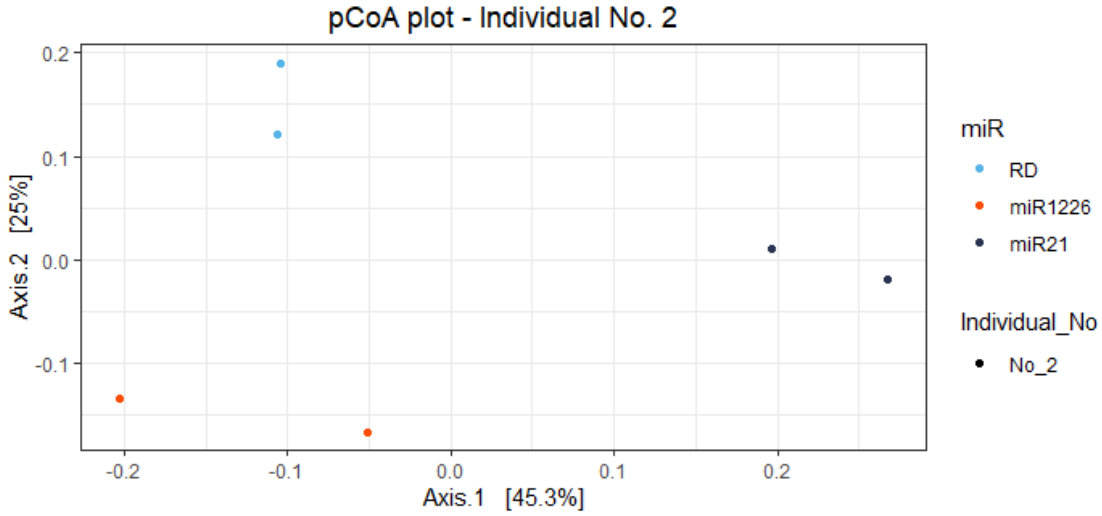
pCoA plot - Individual No. 2
Axis.2 [25%]
Axis.1 [45.3%]
0.2
0.1
0.0
-0.1
-0.2
-0.1
0.0
0.1
0.2
miR
RD
miR1226
miR21
Individual_No
No_2

C

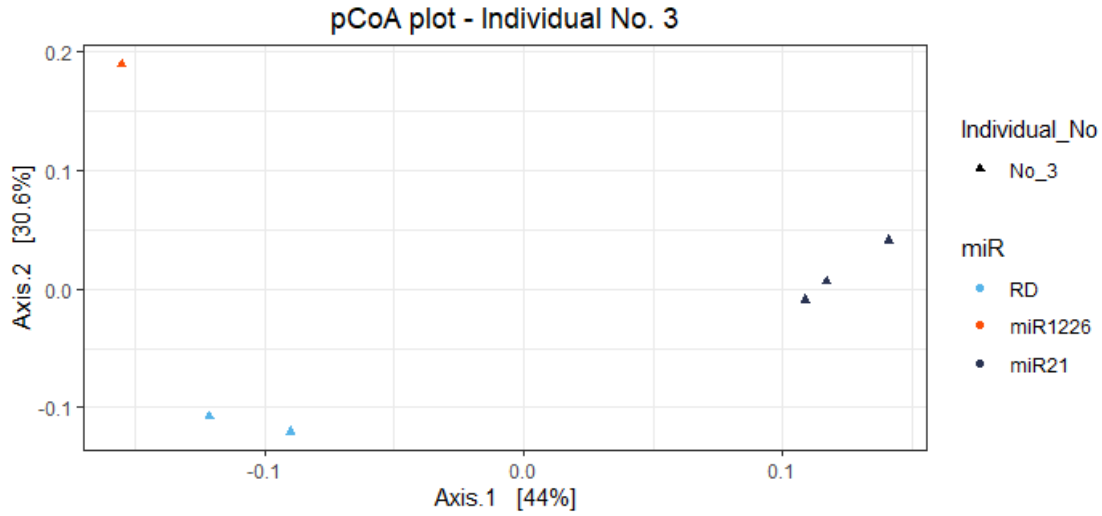
pCoA plot - Individual No. 3
Axis.2 [30.6%]
Axis.1 [44%]
0.2
0.1
0.0
-0.1
-0.1
0.0
0.1
Individual_No
No_3
miR
RD
miR1226
miR21

D

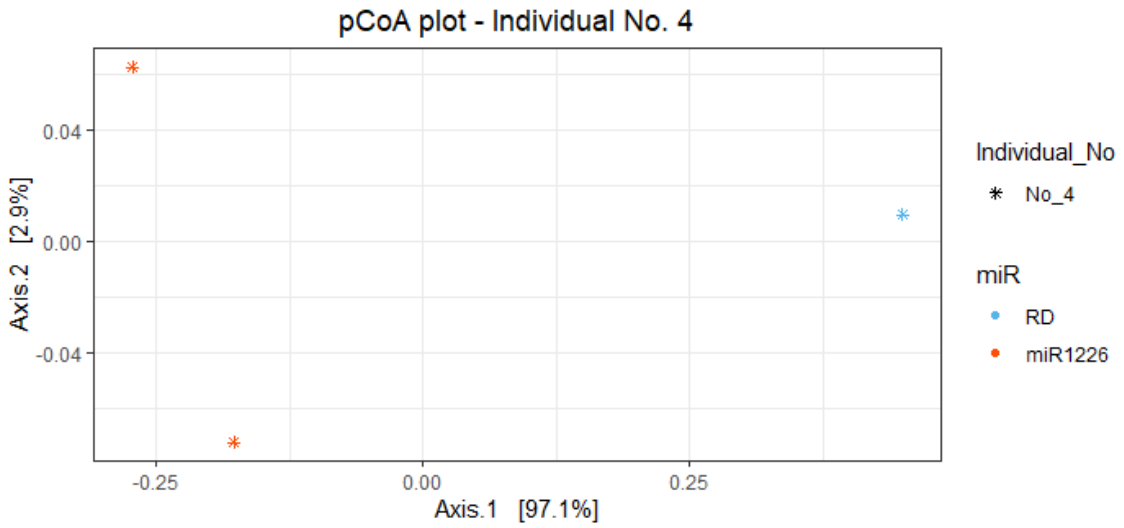

Figure 7. Principal coordinate analysis (pCoA) (based on Bray-Curtis distance matrix) representing β-diversity within analysed individuals (A-D). Individual number is represented by shape and sample type is represented by color.

Bar charts indicating the relative abundance of different bacterial taxa at the phylum level from the faecal samples of 4 analysed individuals are presented in the Figure 8.

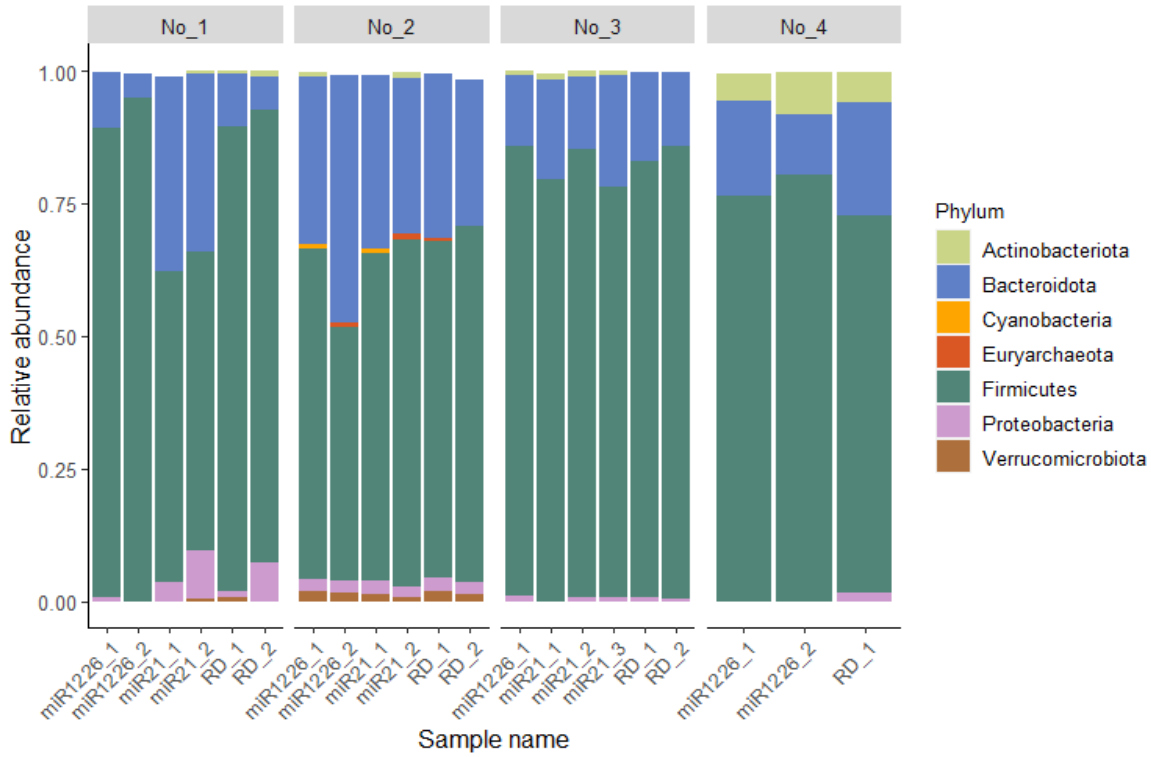

Figure 8. Relative abundance of bacteria interacting with supplemented miRNAs in FACS sorted fractions from the faeces of 4 analyzed individuals classified at the phylum level. For each individual the fractions were sorted based on which organisms detected in faeces take up supplemented miR-1226, miR-21. Randomly sorted fractions (RD) provide insight into the overall microbiota constitution in each analysed individual.

Firmicutes are the dominating phylum in each individual as well as Bacteroidota, though to a lesser extent. Same trends in microbiome composition have been reported by the Human Microbiome Project (Human Microbiome Project Consortium, 2012). Individual No 4 also contains more of Actinobacteriota than other analysed individuals. At the phylum level there are no major observable differences in composition of sorted fractions, except for Individual 1, where an increase in relative abundance of Bacteroidota is detected in miR21 sorted fractions.

It was then looked at the relative abundance of gut bacteria at the family level (Figure 9). The differences in bacteria composition among different fractions is best observed visually in individuals No. 1 and No. 4 in miR-1226 samples when compared to randomly sorted fractions acquired from the same individual. There is a significant increase in Ruminococcaceae and a decrease in Lachnospiraceae families. Such significant differences in sorted fractions and its replicates supports data from confocal microscopy analysis that showed colocalization of fluorescently labelled miRs and rod-shaped bacteria, which could be attributable to Ruminococcacae. In miR-21 sorted fractions there seem to be an increase in Oscillospiraceae in individuals No. 2 and No. 3, although not to the same extent as seen for Ruminococcaceae in miR-1226 fractions.

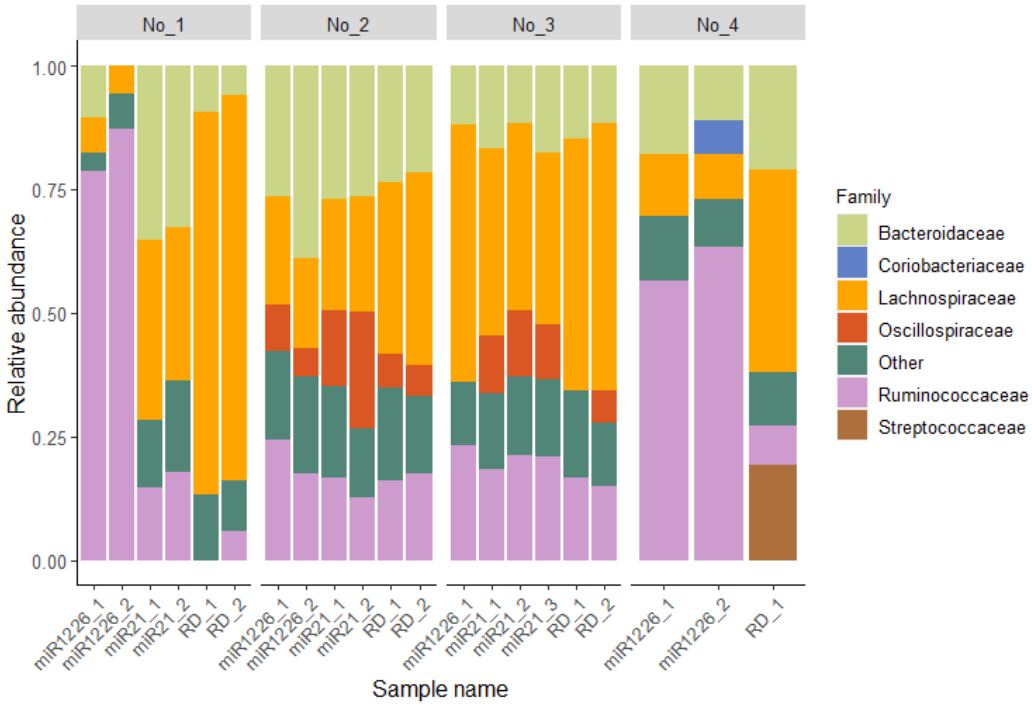

Figure 9. Relative abundance of bacteria interacting with supplemented miRNAs in FACS sorted fractions from the faeces of 4 analyzed individuals classified at the family level. For each individual fractions were sorted based on what organisms take up

supplemented miR-1226, miR-21. Randomly sorted fractions (RD) provide insight into the overall composition of the microbiota in (untargeted) sorted fractions of each analysed individual.

Afterwards, a differential abundance analysis using DESeq2 was performed to illustrate quantitatively which bacteria is enriched or depleted in the analysed miR-specific fractions compared to RD samples from the same individual. An ASV with a log 2 fold change >2 is considered significantly enriched, while ASVs with log 2 fold change <2 are significantly depleted. For either case, only significant changes ($p<0.05$) are reported. A list of selected enriched ASVs as presented in the Figure 10 for miR-21 samples (panels A-C) and Figure 11 for miR-1226 samples (panels A-D) is further summarized in the Table 3 for miR-21 and miR-1226 samples respectively.

A

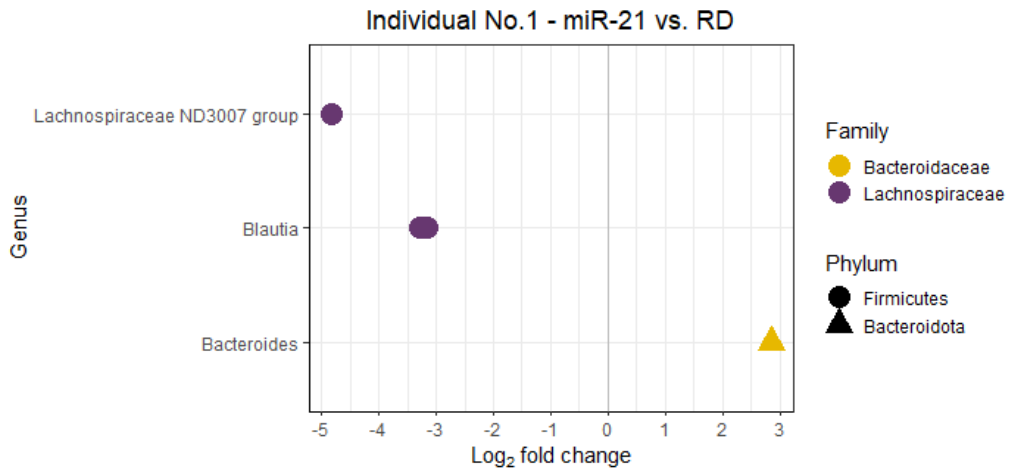

B

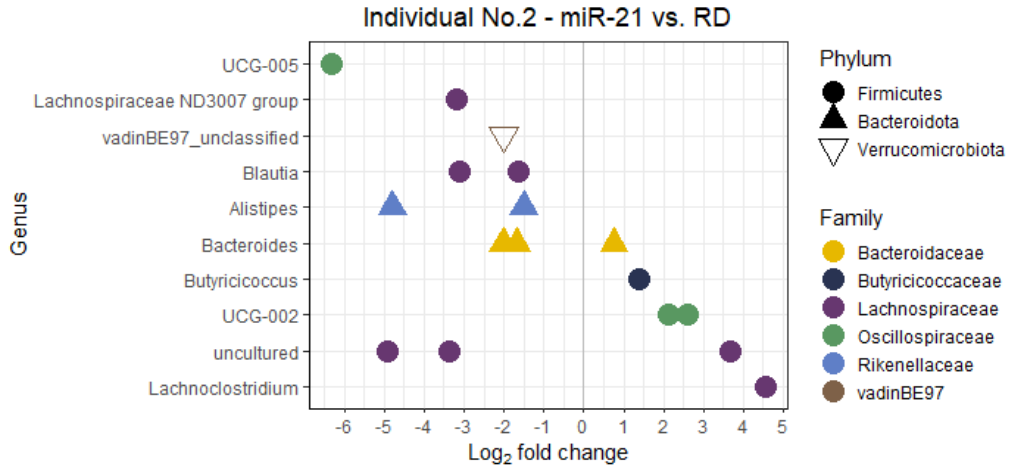

C

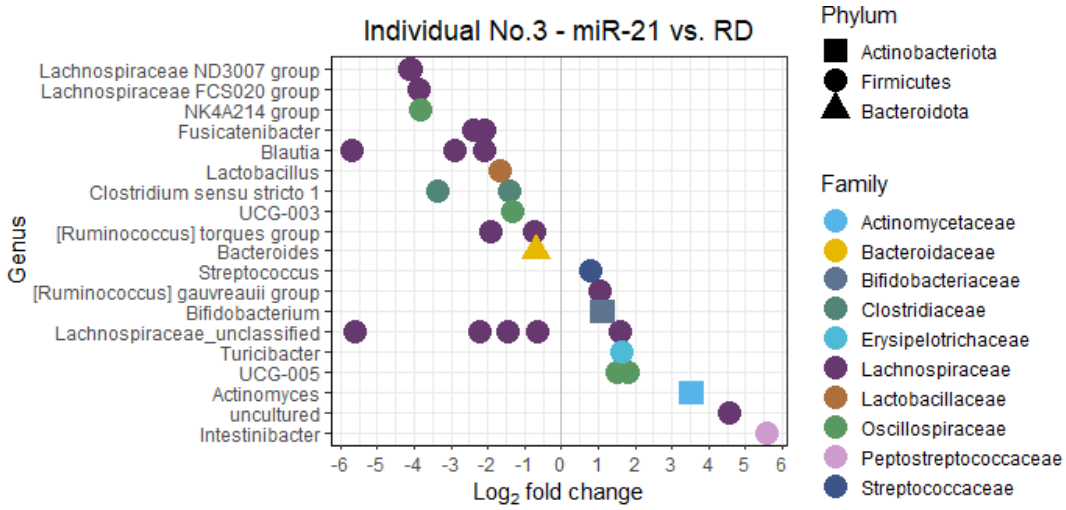

Figure 10. Differential abundance analysis using deseq2 for miR-21 in analyzed individuals 1-3 (A-C). Each dot on the graph is an ASV, grouped by genus (y axis), colored by family and shaped by phylum. The x axis represents log 2 fold change in the abundance levels.

In miR-21 sorted fractions Firmicutes are the most affected by both being enriched or depleted, while Bacteroidota is only enriched in one of the analysed subjects suggesting that either Bacteroides do not respond to the presence of miR-21 as sensitively as Firmicutes do or the effect is not so prominent due to lower overall abundance of Bacteroidota. Within Firmicutes, for Individuals 2-4 there is an increase in several unclassified Oscillospiraceae genera while others are decreased. Differential abundance analysis has been repeated for miR-1226 sorted fractions and its results are given in the Figure 11, panels A-D.

A

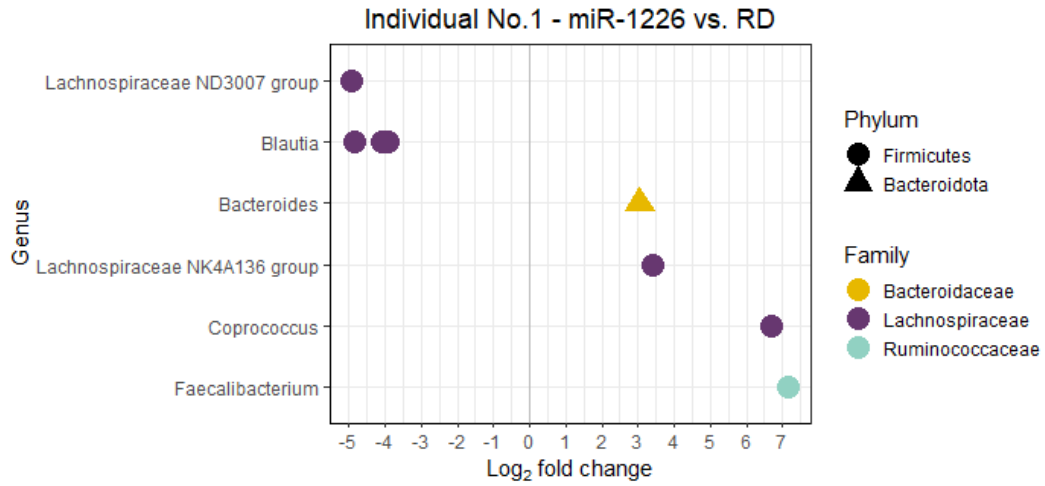

B

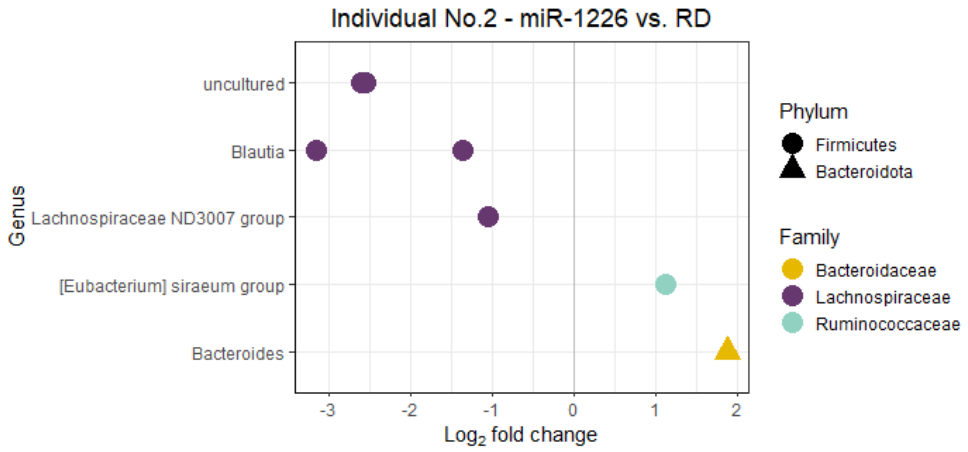

C

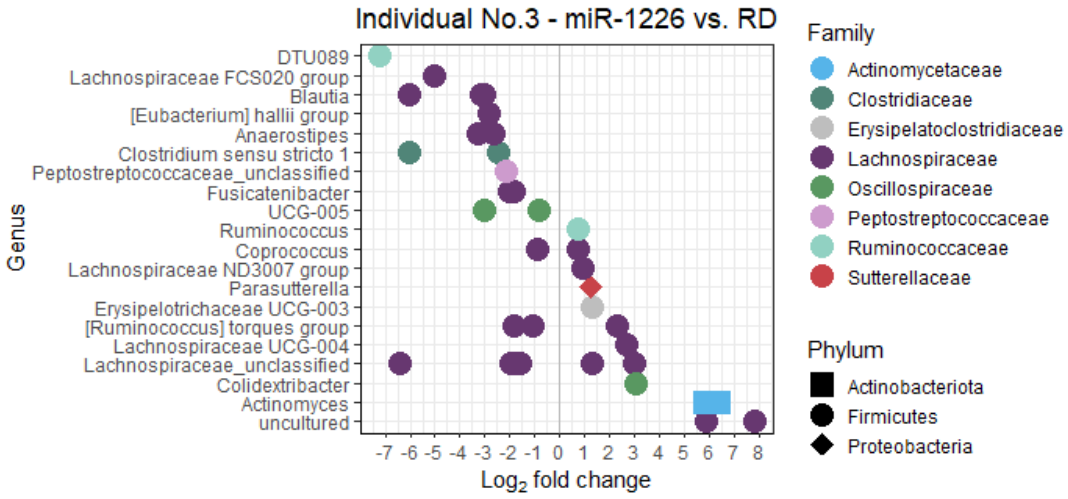

D

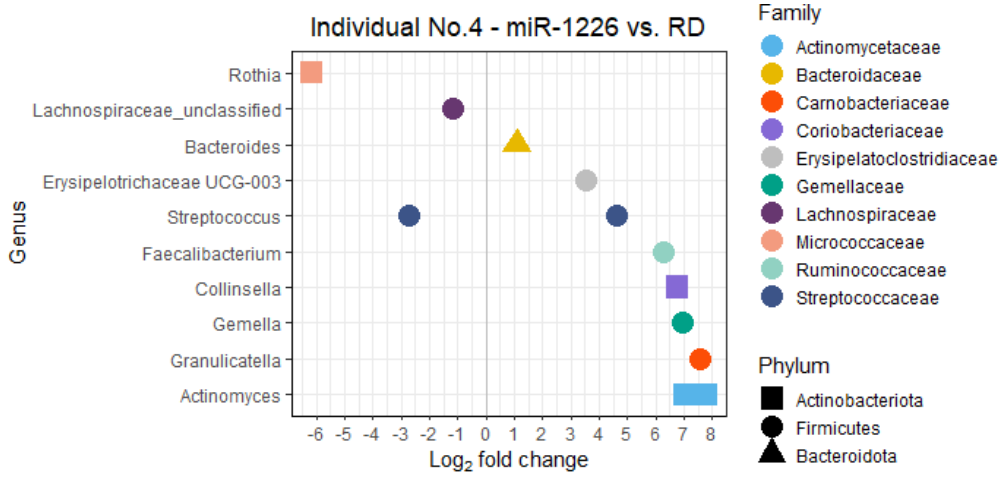

Figure 11. Differential abundance analysis using deseq2 for miR-1226 in analyzed individuals 1-4 (A-D). Each dot on the graph is an ASV, grouped by genus (y axis), colored by family and shaped by phylum. The x axis represents log 2 fold change in the abundance levels.

Depletion in Lachnospiraceae and increase in Actinomycetaceae, Ruminococacceae and Lachnospiraceae and *Bacteroides* are seen in miR-1226 sorted fractions. Individual No. 4 had a greater variability of enriched bacteria interacting with fluorescently labeled miR-1226 as opposed to depletion/enrichment effects observed in other individuals on different Lachnospiraceae genera. Overall, it seems that different genera of Lachnospiraceae, Rumicoccaceae and *Bacteroides* are most susceptible to interaction with miRs.

A list of enriched ASVs (log2fold change >2, as presented in the Figures 10, 11) is summarized and given in the Table 3. Each assorted sequence variant (ASV) had its sequence blasted to NCBI database to elucidate species with most similar sequences to the query.

MiR-1226							
ASV	**Ind No**	**log2 Fold Change**	**P val**	**Family**	**Genus**	**NCBI BLAST**	**Seq. similarity**
ASV_sdd_9s7	No_1	7.173	0.006	Ruminococcaceae	Faecalibacterium	Faecalibacterium prausnitzii strain ATCC 27768	98.81%
ASV_bzl_wzp	No_1	6.677	0.000	Lachnospiraceae	Coprococcus	Coprococcus catus strain VPI-C6-61	99.21%
ASV_iq1_sq3	No_1	3.406	0.000	Lachnospiraceae	Lachnospiraceae NK4A136 group	Bacteroides xylanolyticus strain X5-1	98.02%
ASV_g1t_iba	No_1	3.043	0.001	Bacteroidaceae	Bacteroides	Bacteroides faecichinchillae JCM 17102/ Bacteroides thetaiotaomicron strain VPI-5482	100.00%
ASV_dxn_i2u	No_3	7.783	0.000	Lachnospiraceae	uncultured	Merdimonas faecis strain BR31	95.65%
ASV_dzg_d34	No_3	6.393	0.000	Actinomycetaceae	Actinomyces	Schaalia odontolytica strain CCUG 20536	100.00%
ASV_46t_jjz	No_3	5.862	0.002	Lachnospiraceae	uncultured	Hungatella effluvii strain UB-B.2	96.05%
ASV_l8s_yli	No_3	5.839	0.012	Actinomycetaceae	Actinomyces	Schaalia odontolytica strain CCUG 20536	99.60%
ASV_dcs_ypy	No_3	3.048	0.000	Oscillospiraceae	Colidextribacter	Colidextribacter massiliensis strain Marseille-P3083	97.63%
ASV_pzj_k2y	No_3	3.001	0.001	Lachnospiraceae	Lachnospiraceae_ unclassified	[Clostridium] bolteae strain 16351	95.29%
ASV_ey9_gs8	No_3	2.672	0.005	Lachnospiraceae	Lachnospiraceae UCG-004	[Clostridium] aldenense strain RMA 9741	95.26%
ASV_mn8_8fd	No_3	2.286	0.004	Lachnospiraceae	[Ruminococcus] torques group	Ruminococcus faecis JCM 15917 strain Eg2	99.60%
ASV_dzg_d34	No_4	7.797	0.000	Actinomycetaceae	Actinomyces	Schaalia odontolytica strain CCUG 20536	100.00%
ASV_3oh_hs2	No_4	7.558	0.002	Carnobacteriaceae	Granulicatella	Granulicatella adiacens strain GIFU 12706	99.60%
ASV_l8s_yli	No_4	7.044	0.000	Actinomycetaceae	Actinomyces	Schaalia odontolytica strain CCUG 20536	99.60%
ASV_a8z_y3c	No_4	6.950	0.000	Gemellaceae	Gemella	Gemella sanguinis strain 2045-94	100.00%
ASV_p2f_btm	No_4	6.757	0.000	Coriobacteriaceae	Collinsella	Collinsella aerofaciens strain JCM 10188	100.00%
ASV_sdd_9s7	No_4	6.304	0.001	Ruminococcaceae	Faecalibacterium	Faecalibacterium prausnitzii strain ATCC 27768	98.81%
ASV_71w_7js	No_4	4.614	0.000	Streptococcaceae	Streptococcus	Streptococcus gordonii strain NCTC7865	100.00%

ASV_qvd_ehk	No_4	3.561	0.000	Erysipelatoclostridiaceae	Erysipelotrichaceae UCG-003	Longibaculum muris strain MT10-315-CC-1.2-2	93.36%
MiR-21							
ASV_g1t_iba	No_1	2.853	0.002	Bacteroidaceae	Bacteroides	Bacteroides faecichinchillae JCM 17102/ Bacteroides thetaiotaomicron strain VPI-5482	100%
ASV_9f1_37k	No_2	2.137	0.000	Oscillospiraceae	UCG-002	Oscillibacter valericigenes strain Sjm18-20	94.49%
ASV_c6l_koa	No_2	2.612	0.000	Oscillospiraceae	UCG-002	Oscillibacter valericigenes strain Sjm18-20	93.07%
ASV_66p_922	No_2	3.667	0.001	Lachnospiraceae	uncultured	[Clostridium] algidixylanolyticum strain SPL73	96.84%
ASV_9h2_dff	No_2	4.556	0.001	Lachnospiraceae	Lachnoclostridium	Kineothrix alysoides strain KNHs209	98.02%
ASV_711_hlc	No_3	5.556	0.002	Peptostreptococcaceae	Intestinibacter	Intestinibacter bartlettii strain WAL 16138	98.81%
ASV_dzg_d34	No_3	3.541	0.003	Actinomycetaceae	Actinomyces	Schaalia odontolytica strain CCUG 20536	100%
ASV_dxn_i2u	No_3	4.567	0.006	Lachnospiraceae	uncultured	Merdimonas faecis strain BR31	95.65%

Table 3. Summary of significantly enriched ASVs acquired from differential abundance analysis for fluorescently labelled and sorted miR-1226 and miR-21 fractions. Most similar 16S sequences to acquired ASVs have been searched for in https://www.ncbi.nlm.nih.gov database.

As shown in Table 3, in miR-1226 sorted fractions, the ASVs with high (>98%) sequence similarities with sequences in the database are identical to *Bacteroides faecichinchillae/thetaiotaomicron*, *Bacteroides xylanolyticus, Ruminococcus faecis, Streptococcus gordonii, Schaalia odontolytica*, *Gamella sarguins*, *Collinsella aerofaciens*, *Coprococcus catus*, *Faecalibacterium prausnitzii*. In miR-21 sorted fractions, the ASVs with high (>98%) sequence similarities with sequences in the database are the ones identical to *Bacteroides faecichinchillae/thetaiotaomicron*, *Schaalia odontolytica*, *Kineothrix alysoides* and *Intestinibacter bartlettii*. Out of this list, six bacterial species (summarized on Table 2) have been selected for further culture growth experiments, based on availability, easiness to culture and sequence similarity.

To sum up data acquired in the experimental part 1, it can be stated that confocal microscopy images showed overlap between fecal bacteria and miR-1226, and to a less extent with miR-21, suggesting co-localization and potential uptake of fluorescently labelled miR-1226. Further analysis through sequencing of fluorescently activated cell sorted fractions suggested that there is specificity in this interaction, to some degree: α-diversity results of collected fractions after sequencing showed that miR-1226 sorted samples from most individual, but not miR21 samples, have decreased diversity compared to RD samples, indicating that it may be up-taken by less diverse bacterial communities than those interacting with miR-21. β-diversity and pCoA analysis highlighted that there are greater differences in the community composition among miR-specific sample types acquired from different individuals. Differential abundance

analyses showed that Firmicutes are the dominating phylum in all analysed individuals, and that overall *Bacteroides* and bacteria in families Lachnospiraceae, Ruminoccocaeae, Oscillospiraceae and Actinomycetaceae are responding to supplemented miRNAs more often than other bacterial families.

3.2 Experimental part 2- Impact of miRNA supplementation on bacterial growth *in vitro*

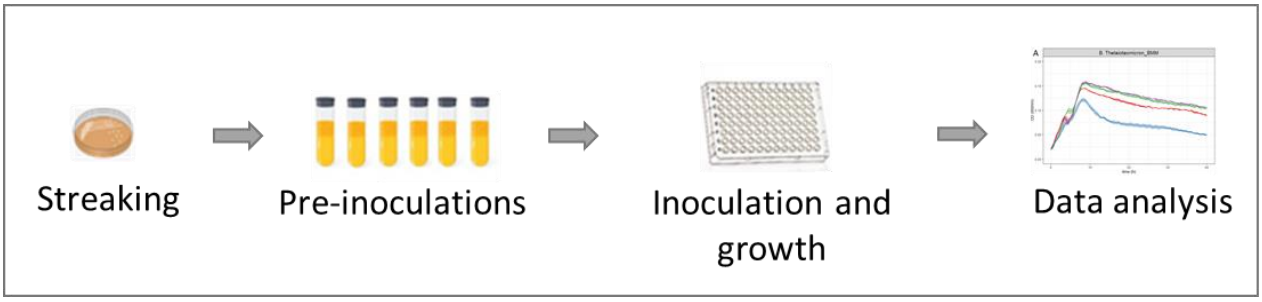

Figure 12. Schematic representation of Experimental part 2 - evaluation of miRNA induced effect on bacterial growth in vitro.

For the assessment of the effect supplemented miRNAs could have on the growth of pure cultures, the following bacteria strains have been selected (details of selection in Experimental part 1): *Bacteroides thetaiotaomicron, Bacteroides finegoldii, Collinsella aerofaciens, Feacalibacterium prausnitzii and Coprococcus catus*. Effect of added miRNAs was to be assessed by analyzing the growth patterns of selected bacterial strains (Figure 12) in different media – YCFA, BHI and BMM (Bacteroides minimal media) as detailed in the Methods section, Table 2.

Each culture was subjected to a colony PCR or DNA extraction and Sanger sequencing of its 16S rRNA gene to confirm colony's homogeneity and identity. *Collinsella aerofaciens* and *Ruminococcus gnavus* were provided by Dr. Michaela Lang (AKH, Vienna) with already confirmed identity. Once the identity of bacterial culture has been confirmed, the growth of bacteria with supplemented miR-21, miR-1226, DEPC water and a sequence from *Arabidopsis thaliana* (negative control) was investigated by measuring the optical density (OD) at 600 nm of each strain inoculated in liquid medium.

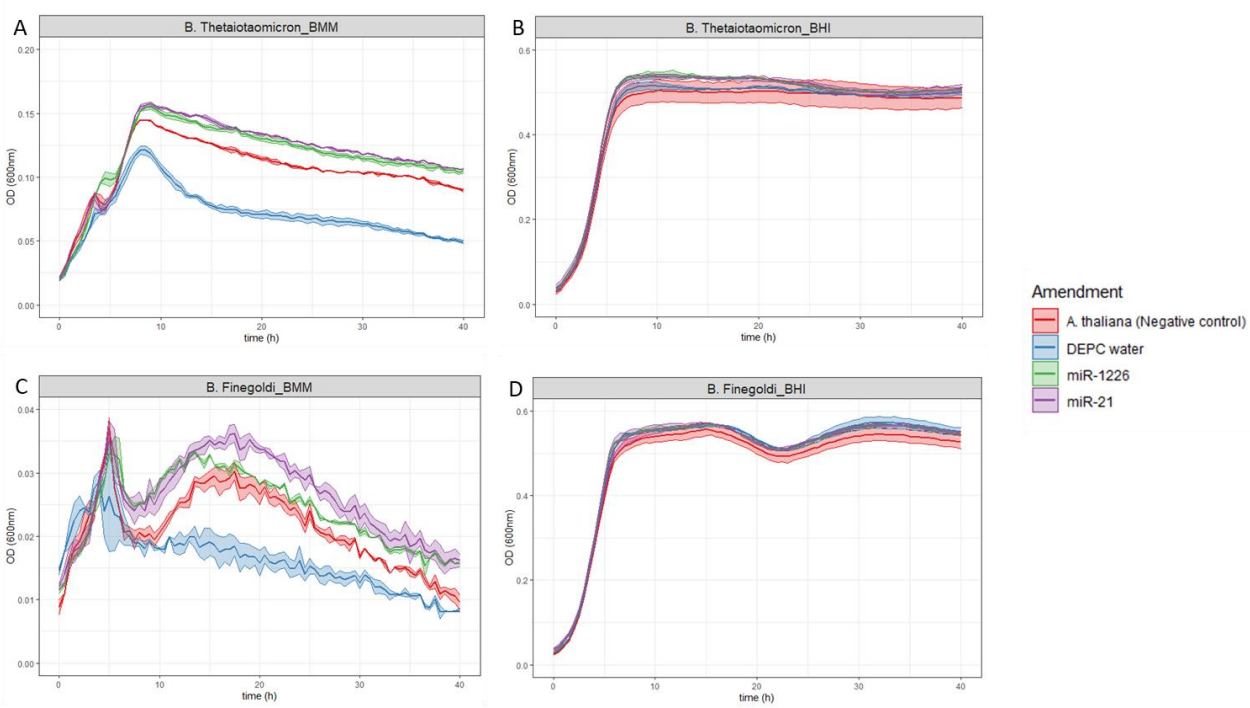

Figure 13. Growth of B. thetaiotaomicron and B. finegoldii in BMM (A,C) and BHI (B,D) with 1.25 µM of supplemented miR-1226 (green), miR-21 (purple), A. thaliana (negative control) (red) and DEPC water (blue). Growth rates were observed for 40 hours, measuring optical density (OD at 600nm) every 30 minutes. Average of three different replicates is shown in a line with darker color, and shaded areas represent standard deviation.

Figure 13 shows growth of *B. thetaiotaomicron* and *B. finegoldii* in Bacteroides minimal media (BMM) (panels A-B) and BHI (panels C-D) with 1.25 µM of supplemented miR. Strains grown in BHI appear to have no significant effect of the supplemented miRNAs on its growth rates potentially due to high availability of nutrients, whereas the growth rates of supplemented strains cultured in BMM did start to diverge after approximately 5 hours of incubation. Growth of *B. thetaiotaomicron* and *B. finegoldii* seems preferentially boosted by miR-21, followed by miR-1226. A sequence from *A. thaliana* increase the growth rates of both Bacteroides strains but less than miR-1226 and miR-21 supplemented samples (Figure 13). This indicates that miRNA may have an effect at the gene level on the growth rates of analysed Bacteroides under certain stressful conditions. Moreover, changes in growth rates seem to be delayed and only activated after a period of time. That may be attributable to a decreased availability of nutrients in Bacteroides minimal media, a possible need to switch metabolic pathways or to avoid harmful build-up of toxic by-products - all forcing the bacteria to adopt new survival strategies, potentially utilizing miRNAs to alter its gene expression. Since both strains grow better in the presence of added miRNAs (even negative controls) it could also be hypothesized that bacteria degrade added miRNAs and use it as a source of nutrition. However, increased growth rates of miR-21 and miR-1226 when compared to negative control, suggest

that added miRNAs may indeed have a role in altered gene expression, which will be further investigated by transcriptomic analyses in the future.

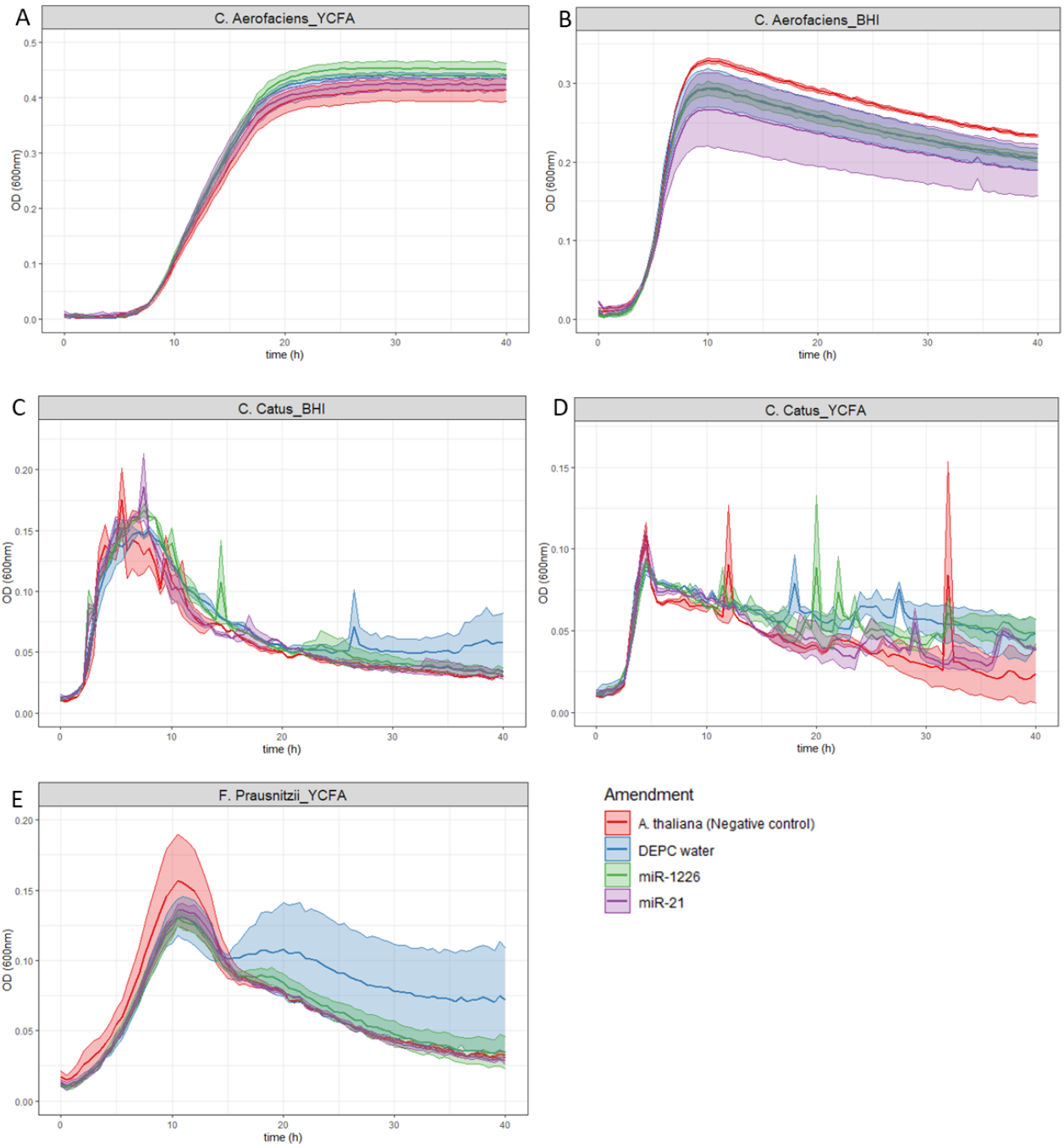

Figure 14. Growth of C. aerofaciens in YCFA (A) and BHI (B), C. catus in BHI (C) and YCFA (D), F. prausnitzii in YCFA (E) with 1.25 µM of supplemented miR-1226 (green), miR-21 (purple), A. thaliana (negative control) (red) and DEPC water (blue). Growth rates were observed for 40 hours, measuring optical density (OD at 600nm) every 30 minutes. Average of two different replicates is shown in a line with darker color, and shaded areas represent standard deviation.

Figure 14, panels A-E, shows the growth of *C. aerofaciens, C. catus and F. prausnitzii* in YCFA and BHI as averages of two technical replicates. Overall, no major impact of the miRs on the growth of these organisms could be observed. *C. catus* grown in both mediums exhibit spikes in growth curves which may be attributable to its ability to form biofilms that eventually aggravates the optical density measurements and makes the data unreliable. It suggests that experimental setup should be adjusted to biofilm forming species and growth should be measured not in a 96-well plate but rather in the test tubes, as that would allow more vigorous shaking and less interference of the biofilms to the measurement. *C. aerofaciens* grown in BHI and *F. prausnitzii* grown in YCFA had significant degree of variation between its replicates overlapping the growth curves of different amendments thus questioning the credibility of the acquired data. *C. aerofaciens* grown in YCFA seemed not to be affected by addition of different miRNAs or negative control. It would be of interest to adjust the media and limit its nutrients, as for *Bacteroides* medium, to see whether the same patterns detected for the rich medium are kept.

3.3 Experimental part 3 - Comparison of miRNA abundance in faeces of healthy individuals and patients suffering from inflammatory bowel diseases.

The aim of Experimental part 3 was to evaluate feacal miRNA abundance profiles in different individuals and compare the abundance levels among healthy subjects versus those suffering from inflammatory bowel disease. This initial screening of few candidate miRs would serve as a basis for future work in which selected samples and miRs (based on their miR profiles, as assessed by qPCR) would be selected for further miRNA deep sequencing and investigation. For this purpose faecal samples have been collected with consent from a group of healthy volunteers and immediately frozen at -80°C. Samples of inflammatory bowel disease patients were obtained from the Vienna General Hospital (AKH) at the courtesy of Dr. Michaela Lang. The IBD cohort consisted of healthy patients who had colonoscopy performed (controls) but no further indications of disease, and those diagnosed with UC or IBS. Table 4 indicates the state of disease affecting each individual and also whether a biofilm was found covering the cecum and/or ileum of these patients. Each faecal sample (0.2 g of stool) was subjected to RNA extraction and purification. The integrity of the purified RNA was confirmed by agarose gel electrophoresis to be of suitable quality for further analysis because both ribosomal bands 16S and 23S were present and in most cases a high molecular weight band (indicative of the presence of DNA) was absent.

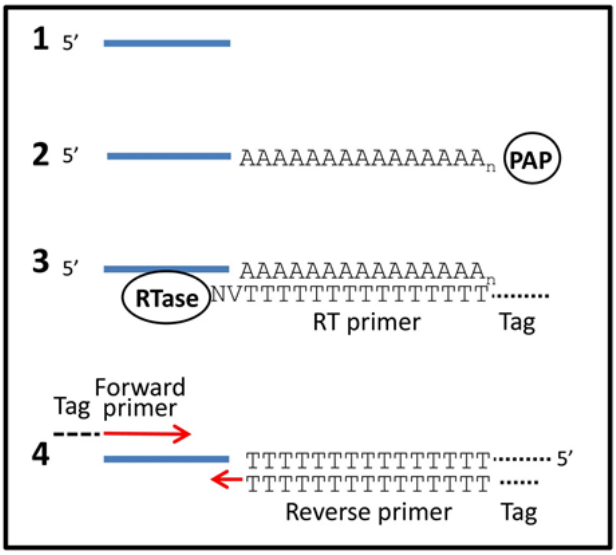

Figure 15. qPCR strategy employed in experimental part 3 - (adapted from Balcells et al, 2011). RNA was polyadenylated by PAP enzyme and transcribed into cDNA using Reverse transciptase and RT primer. qPCR was performed using miR-specific primers as indicated in Table 1.

Isolated RNA (1.5 µg per sample) was then polyadenylated and reverse transcribed (RT) into cDNA, followed by qPCR (Figure 15) for each analysed miRNA targeted with the primers presented in Table 1 (Balcells *et al*., 2011). Initially it was attempted to investigate 11 miRNAs, unfortunately PCR amplification efficiency was often out of optimal 80-115% range. One of the potential causes could have been a PCR reaction inhibition. RNA was extracted using phenol (also known as PCR inhibitor) and the samples may not have been completely phenol-free afterwards interfering with the results. Non-optimal concentration of salts, such as magnesium chloride may have had a negative effect too. Melting temperatures were adjusted and reaction mixtures were supplemented with BSA for better results, however these measures did not yielded a better result. Therefore due to time and resource constraints only 5 specific miRNAs (miR-30d, miR-1246, miR-1226, miR-320e, miR-21) have been selected for the final study. These miRNAs have been selected based on literature indicating their high abundance in faecal samples, and some have been previously implicated in IBD and/or colorectal cancer, as mentioned earlier.

PATIENT CODE	STATE OF DISEASE	BIOFILM IN ILEUM & CECUM
IBDc 1	Control	No
IBDc 4	Control	No
IBDc 5	Control	No
IBDc 7	Control	No
IBDc 11	IBS	Yes
IBDc 13	IBS	Yes
IBDc 9	IBS	Yes
IBDc 10	IBS	No
IBDc 12	IBS	No
IBDc 2	IBS	No
IBDc 3	UC	No
IBDc 6	UC	No

Table 4. Faecal samples acquired from patients with a given code, state of disease and indication of the presence of biofilm in ileum and cecum. IBS refers to inflammatory bowel syndrome, UC – ulcerative colitis.

The abundance levels of 5 miRNAs have been quantified in all analysed samples and compared in the context of disease condition. Abundance levels have been calculated using ΔΔCt method and compared against the levels of miR-26b and eventually expressed as fold over mean control. MiR-26b was selected as an endogenous control due to its high stability and previous indication in the literature of its suitability as a normalization control and coherence among different samples (Link *et al*, 2010).

First of all, all miRNA abundance levels in healthy cohort and IBD cohort have been compared (Figure 16). Wilcoxon statistical analysis showed no significant difference between the two analysed groups. The variability among the samples within the

group is greater in IBD cohort than in the healthy cohort, however there is no significant difference between the variances in the two groups (Pvalue=0.13, Levene's test for equality of variance).

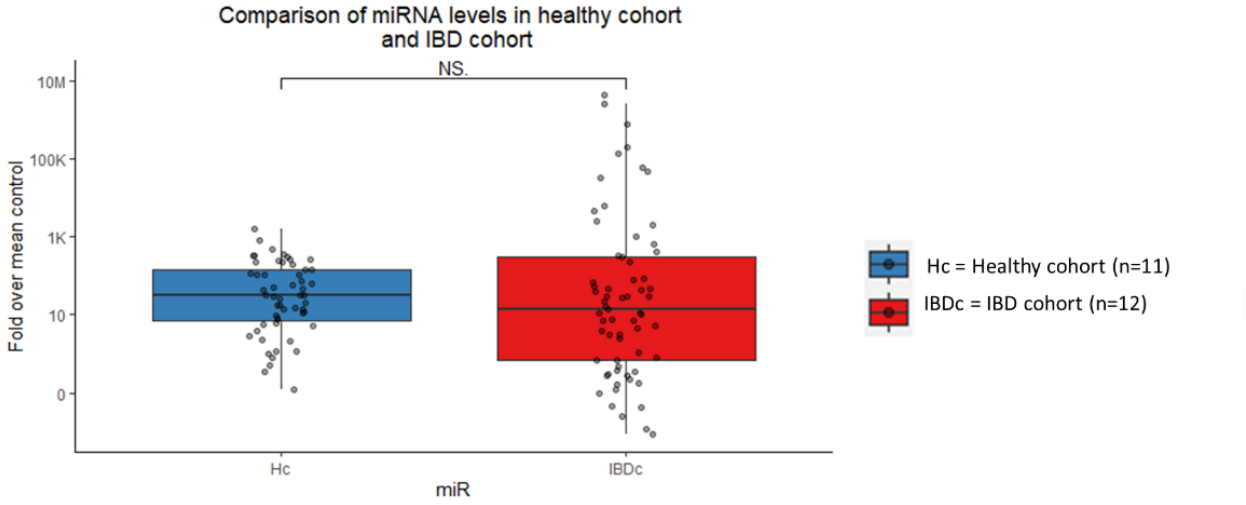

Figure 16. Overall distribution of all miRNA abundance levels investigated in healthy and IBD cohorts. Significance was calculated using Wilcoxon test with a 95% confidence interval.

Next, miRNA abundance levels have been compared for each miRNA among healthy cohort, IBD patients and IBD controls (Figure 17). The highest degree of variability has been observed in IBD controls. Wilcoxon test indicates that there was a statistically significant difference between healthy cohort and IBD patients in miR-21, miR-30d and miR-320e with decreased abundance in IBD patients. MiR-21 abundance levels were also found to be lower in IBD patients when compared to IBD controls. Data acquired in this study showed an overall trend for decreased abundance of miRs, especially of miR-21, miR-30d and miR-320e in the IBD patients compared with healthy cohort. Previous studies have reported discrepant differences in miR-21 levels, and a decrease in miR-1226 levels in IBD patients compared with healthy controls (Ahmed *et al*, 2009, Schönauen *et al*, 2018, Verdier *et al*, 2020). An increase in IBD cohort size could potentially confirm observed trends. It could also be an indication of insufficient sensitivity of the test and therefore unsuitability to be used for a single patient diagnosis. Unfortunately, the reasons why people in IBD control group had to be tested are unknown. Such additional information would allow to account for differences that may arise when analysing data from people that are in remission or at risk. As Ji *et al* (2018) found a correlation between inflammatory disease severity and some miRNA abundance levels, it could be investigated if changes in miRNA abundance are preceding the onset of the disease before settling to levels observed in IBD patients as that could be one of the reasons for highest variability in IBD control group. IBDc1 (Control) and IBDc2 (IBS) remain as outliers in all five analysed miRNA groups with significantly higher abundances than data in other analysed samples (Figure 17).

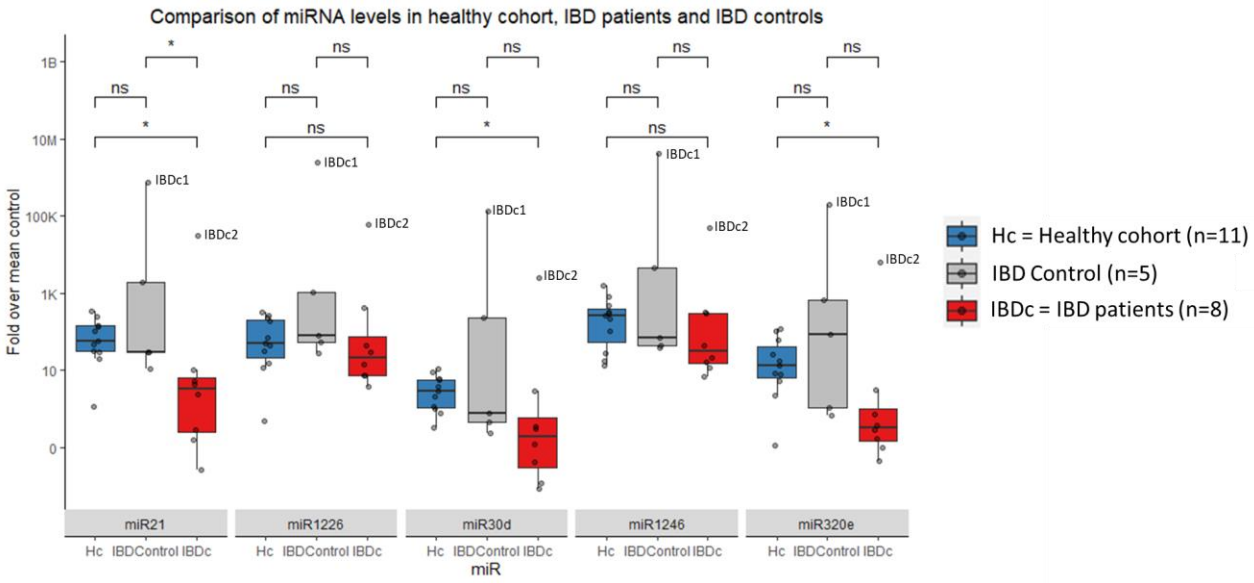

Figure 17. Comparison of miRNA abundance levels between IBD patients, IBD controls and healthy cohort. Significance was calculated using Wilcoxon test with a 95% confidence interval, outlier codes are displayed for better interpretation.

Afterwards, it was looked into the significance of the biofilm found in ileum and cecum of the patient's gut and how it affects the levels of faecal miRNAs. In this case only IBD cohort samples have been used in the comparison. As shown in Figure 18, there is a significant decrease in miR-21 levels in samples with the biofilm, but not in other quantified miRNAs.

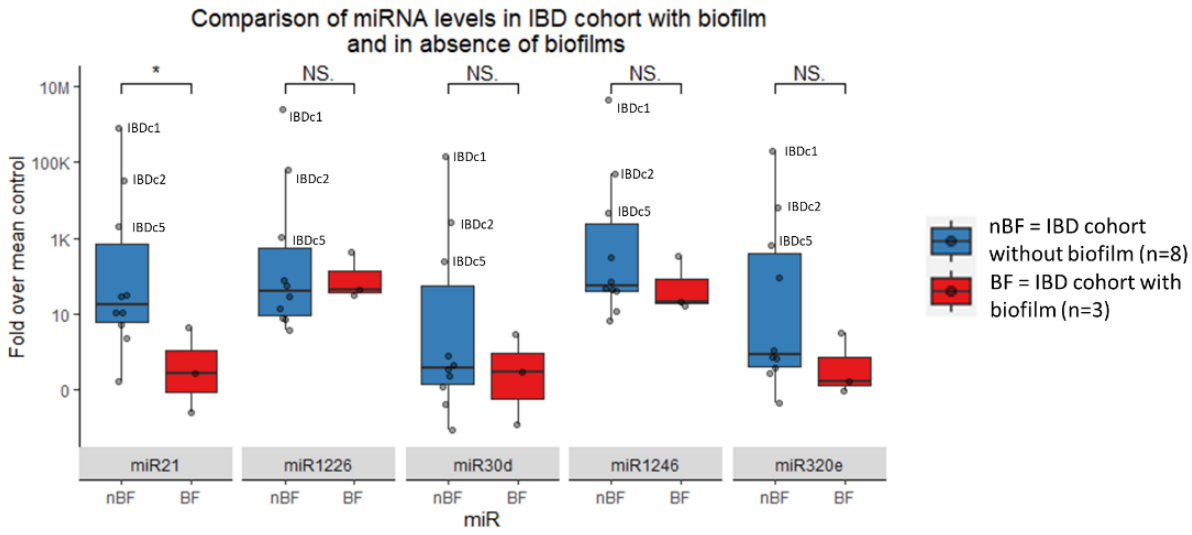

Figure 18. Comparison of miRNA abundance levels between IBD patients with and without the biofilm forming in the gut. Significance was calculated using Wilcoxon test with a 95% confidence interval, outliers are marked to indicate which sample it was acquired from.

Comparison of miRNA abundance levels in UC patients and IBD controls using Wilcoxon test indicated no significant differences between the two groups, although there is a trend for a decrease in levels of all quantified miRNAs in UC patients, except for miR-1246 (Figure 19). These results are in agreement with literature showing that miR-1246 levels tend to be similar among patients with UC and Crohn's disease, but tend to be lower in both conditions compared with control individuals (Schönauen *et al*, 2018). However, more samples/patients would need to be analyzed in order to conclude if acquired results are significant and if trends are reproducible.

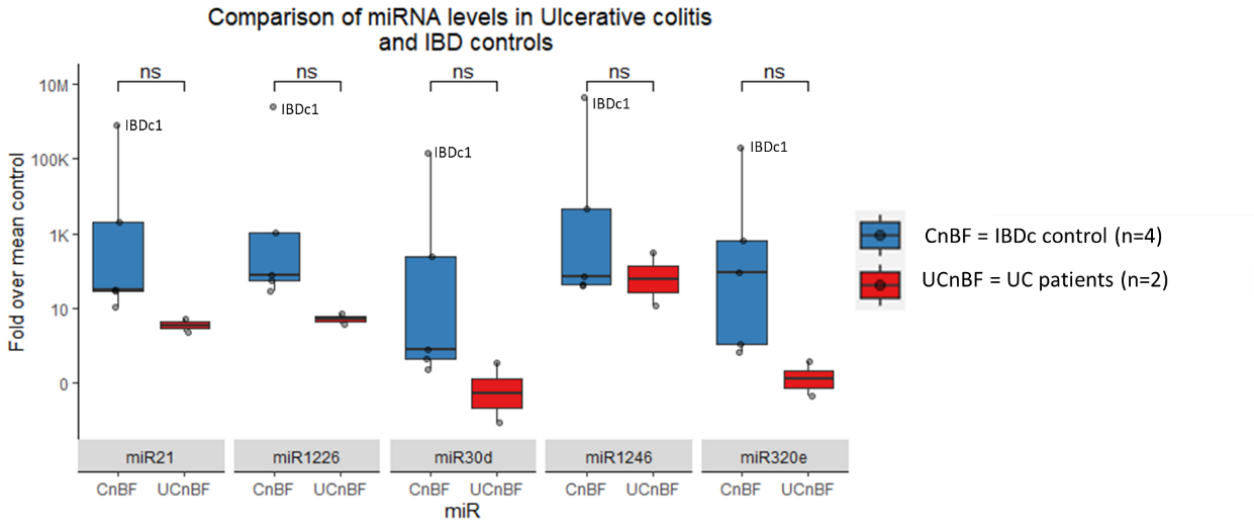

Figure 19. Comparison of miRNA abundance levels between IBD control and IBD patients with ulcerative colitis. Significance was calculated using Wilcoxon test with a 95% confidence interval.

4 Discussion

Interest in human gut microbiota has been growing exponentially in the past years, however there is still not much data describing in detail alterations in microbial abundances and function when analyzing the whole gut community rather than pure, individual cultures. In this study it was investigated whether gut bacteria present in the faecal samples are capable of interacting with the supplemented human microRNAs miR-21 and miR-1226. It was determined through the confocal microscopy that signal from fluorescently labelled miR-1226 colocalizes with the DAPI-stained gut bacteria from the faecal sample thus indicating that miR-1226 enters gut bacteria (Figure 2). It aligns with the work done by Liu *et al* (2016) who showed that miR-1226 but not its scrambled version can increase growth rates of *E. coli* by altering gene expression. Additionally, Liu and colleagues also showed that pure bacteria culture can uptake supplemented fluorescently labelled miRNAs. However, similar experiments done with miR-21 in this study did not yield the same results. Even though miR-21 was found in close proximity to the bacterial cells, there was no overlap observed (Figure 3). Nevertheless, such result could also be influenced by low overall fluorescence of miR-21 levels potentially indicating that it was of compromised quality. Therefore this part of the experiment should be repeated with a different batch of fluorescently labelled miR-21, and also incubating it with fecal sample for longer periods of time before concluding if confocal microscopy images prove that gut bacteria can uptake miR-21.

Fluorescence-activated cell sorting to separate gut bacteria interacting with either fluorescently labelled miR-1226 or miR-21 and further investigation of acquired samples through 16S rRNA sequencing indicated, that in miR-21 sorted fractions most enriched bacterial families were Lachnospiraceae, and Oscillospiraceae. In miR-1226 sorted fractions the most significant enrichment was detected in Lachnospiraceae, Ruminoccocaceae, Bacteroidaceae and Actinomycetaceae. Most decreased bacterial family was various genera of Lachnospiraceae in both miR-21 and miR-1226 samples, especially *Blautia*, which was significantly depleted in the majority of the samples indicating that it tends either not to interact with supplemented miRs or miRs could have an indirect inhibitory effect on its functions. Since *Blautia* has been shown to be involved in gut inflammatory processes (Vacca *et al*, 2020), its inhibition could have significant implications on human health. Therefore it would be interesting to test directly in the future if miRs can inhibit the growth of *Blautia* species. Overall, differential abundance analysis suggests that in gut microbiota there must be a variety of bacterial species that interact with miR-21 and miR-1226, and that this interaction is individual-specific (Figures 10 and 11). This conclusion is supported

by alpha diversities' data, which only indicated decreased diversity among miR specific fractions compared to randomly sorted fractions if analysed individual by individual.

Age, sex, health status, mode of delivery, individual specific genetic variants influence microbial community composition, which may prevent systematic links between specific bacterial species and supplemented miRNAs to be established. Performing growth experiments on pure cultures did help to remove some roadblocks of this type. Pure bacteria cultures have been selected from the list of most enriched bacterial ASVs in miR-associated fractions, as determined from the differential abundance analysis. It was found that rich media may conceal the effect miRNA may have on the growth of bacterial culture, as results from the bacteria grown in bacteroides minimal media revealed differences masked by growth in rich BHI medium. Causing bacteria stress by culturing it in nutrient limited environment may be one of the aspects triggering miRNA effects on analysed cultures. *B. thetaiotaomicron* and *B. finegoldii* grown in BMM have shown increase in growth rates in all samples where miRNAs were supplemented to the culture. It indicates that miRNA could be degraded and utilized as a source of nutrition. However, if miRNA sequences from *Arabidopsis thaliana* (21 bp), miR-21 (22bp) and miR-1226 (26bp) were used as nutrients only, then increase in growth rates would correlate to the length of supplemented miRNA molecule, which was not observed in this experiment. Further investigation would be necessary to determine if there are sequences in the analysed bacterial genome that could be targeted by these miRNA sequences and if gene expression is altered by the presence of miRNA in the culture.

Comparative analysis of miRNA abundance levels among faecal samples of healthy individuals, patients suffering from inflammatory bowel diseases and individuals who were tested although not diseased showed a significant decrease in levels of miR-21, miR-30d, miR-320e in the IBD patients compared to healthy cohort (Figure 17). In agreement, quantification of faecal miRs in the DSS mouse model has shown generalized decrease in miR levels during colitis (Liu *et al*., 2016). Although several studies have reported increased expression of miR-21 in intestinal tissue, its levels have been found unaltered or decreased in faecal samples from IBD patients by the majority of studies published so far (Ahmed *et al*, 2009, Schönauen *et al*, 2018, Ji *et al*, 2018). One can speculate that changes induced in the microbiota lead to a depletion of this miR from the gut lumen, or that secretion of miRs by gut epithelial cells is overall altered during colitis. Interestingly, miR-21 is significantly decreased in IBD patients with mucosal-associated biofilms when compared with patients without biofilm. As biofilm is an extracellular matrix, its presence may be a physical barrier diminishing abilities of miRNA produced and secreted by the gut epithelial cells

to reach the lumen. However we would expect this to also be the case for other miRs. More patients should be included to confirm these interesting results.

Several outliers in IBD group were consistently detected above the averages of abundance levels in all analysed individuals. These outliers belonged to control and IBS groups. Lee *et al* (2018) suggests that inflammatory condition in gastrointestinal tract can occur in cycles, periodically exacerbating and alleviating the overall status of patient's health. That would indicate that even though patients in the control group do not have an active disease at the moment of sampling, they are predisposed to potentially developing it later in life. In many cases, statistical analysis did not indicate significant differences among the analysed groups, possibly due to low sample numbers. In the future studies, data acquired from bigger cohorts should be evaluated to assess statistical significance more reliably. It would also be beneficial to match sex and age of the analysed subjects to reduce variability caused by group – specific features.

More studies analyzing miRNA effects on gut microbiota in its naturally occurring composition would allow to modulate the usage of miRNAs for therapeutic purposes, just like in the experiment by Liu *et al* (2019), where it has been successfully showed that miR-30d can increase the abundance of *A. muciniphila* and suppress the symptoms of multiple sclerosis. Further attention to development of quantitative tests on miRNA abundance levels would also enable a breakthrough in non-invasive diagnosis methods as miRNA levels have the potential to be used as a biomarker with indication of severity of the disease.

5 References

Ahmed, F.E., Jeffries, C.D., Vos, P.W., Flake, G., Nuovo, G.J., Sinar, D.R., Naziri, W., Marcuard, S.P. (2009) Diagnostic microRNA markers for screening sporadic human colon cancer and active ulcerative colitis in stool and tissue. *Cancer Genomics Proteomics*. **6**:281-95.

Balcells, I., Cirera, S., & Busk, P.K. (2011) Specific and sensitive quantitative RT-PCR of miRNAs with DNA primers. *BMC Biotechnology* **11**: 70.

Bartel, D. P. (2018). Metazoan MicroRNAs. *Cell* **173:** 20–51.

Berg, G., Rybakova, D., Fischer, D., Cernava, T., Champomier Vergès, M.C., Charles, T., Chen, X., Cocolin, L., Eversole, K., Herrero Corral, G., Kazou, M., Kinkel, L., Lange, L., Lima, N., Loy, A., Macklin, J.A., Maguin, E., Mauchline, T., McClure, R., Mitter, B., Ryan, M., Sarand, I., Smidt, H., Schelkle, B., Roume, H., Kiran, G.S., Selvin, J., Soares Correa de Souza, R., van Overbeek, L., Singh, B.K., Wagner, M., Walsh, A., Sessitsch, A., Schloter, M. (2020) Microbiome definition re-visited: old concepts and new challenges. *Microbiome* **8**.

Bohnhoff, M., Miller, C.P. (1962) Enhanced susceptibility to Salmonella infection in streptomycin-treated mice. *The Journal* of *Infectious Diseases* **111**: 117-127.

Cho, J.H., Brant, S.R. (2011) Recent insights into the genetics of inflammatory bowel disease. *Gastroenterology* **140**: 1704-1712.

Darfeuille-Michaud, A., Neut, C., Barnich, N., Lederman, E., Di Martino, P., Desreumaux, P., Gambiez, L., Joly, B., Cortot, A., Colombel, J.F. (1998) Presence of adherent Escherichia coli strains in ileal mucosa of patients with Crohn's disease. *Gastroenterology* **115**: 1405-13.

David, L.A., Maurice, C.F., Carmody, R.N., Gootenberg, D.B., Button, J.E., Wolfe, B.E., Ling, A.V., Devlin, A.S., Varma, Y., Fischbach, M.A., Biddinger, S.B., Dutton, R.J., Turnbaugh, P.J. (2014) Diet rapidly and reproducibly alters the human gut microbiome. *Nature* **23**: 559-63.

Donaldson, G.P., Lee, S.M., Mazmanian, S.K. (2016) Gut biogeography of the bacterial microbiota. *Nature Reviews Microbiology* **14**: 20-32.

Fakhoury, M., Negrulj, R., Mooranian, A., Al-Salami, H. (2014) Inflammatory bowel disease: clinical aspects and treatments. *Journal of Inflammation Research* **7**: 113–120.

Gensollen, T., Iyer, S.S., Kasper, D.L., Blumberg, R.S. (2016) How colonization by microbiota in early life shapes the immune system. *Science* **352**: 539-44.

Geuking, M.B., Cahenzli, J., Lawson, M.A., Ng, D.C., Slack, E., Hapfelmeier, S., McCoy, K.D., Macpherson, A.J. (2011) Intestinal bacterial colonization induces mutualistic regulatory T cell responses. *Immunity.* **34**: 794-806.

Gill, S.R., Pop, M., DeBoy, R.T., Eckburg, P.B., Turnbaugh, P.J., Samuel, B. S., Gordon, J. I., Relman, D. A., Fraser-Liggett, C. M., & Nelson, K. E (2006) Metagenomic analysis of the human distal gut microbiome. *Science* **312**: 1355–1359.

Gkouskou, K.K., Deligianni, C., Tsatsanis, C., Eliopoulos, A.G. (2014) The gut microbiota in mouse models of inflammatory bowel disease. *Frontiers in Cellular and Infection Microbiology* **4**: 28.

Hegstrand, L. R., & Hine, R. J. (1986). Variations of brain histamine levels in germ-free and nephrectomized rats. *Neurochemical research* **11:** 185–191.

Hugon, P., Dufour, J.C., Colson, P., Fournier, P.E., Sallah, K., Raoult, D. (2015) A comprehensive repertoire of prokaryotic species identified in human beings. *The Lancet. Infectious diseases* **15**: 1211-1219.

Human Microbiome Project Consortium. (2012) Structure, function and diversity of the healthy human microbiome. *Nature* **486**: 207–214.

Ji, Y., Li, X., Zhu, Y., Li, N., Zhang, N., Niu, M. (2018) Faecal microRNA as a biomarker of the activity and prognosis of inflammatory bowel diseases. *Biochemical and Biophysical Research Communications* **503**: 2443–50.

Johansson, M.E., Larsson, J.M., Hansson, G.C. (2011) The two mucus layers of colon are organized by the MUC2 mucin, whereas the outer layer is a legislator of host-microbial interactions. *Proceedings of the National Academy of Sciences of the United States of America* **108:** 4659-4665.

Johnston, D.G.W., Williams, M.A., Thaiss, C.A., Cabrera-Rubio, R., Raverdeau, M., McEntee, C., Cotter, P.D., Elinav, E., O'Neill, L.A.J., Corr, S.C. (2018) Loss of MicroRNA-21 Influences the Gut Microbiota, Causing Reduced Susceptibility in a Murine Model of Colitis. *Journal of Crohn's and Colitis* **12**: 835–848.

Khan, I., Ullah, N., Zha, L., Bai, Y., Khan, A., Zhao, T., Che, T., Zhang, C. (2019) Alteration of Gut Microbiota in Inflammatory Bowel Disease (IBD): Cause or Consequence? IBD Treatment Targeting the Gut Microbiome. *Pathogens* **8**: 126.

Lan, H., Lu, H., Wang, X., Jin, H. (2015) MicroRNAs as Potential Biomarkers in Cancer: Opportunities and Challenges, *BioMed Research International* **2015**.

Lee, S.H., Kwon, J.E., Cho, M.L. (2018) Immunological pathogenesis of inflammatory bowel disease. *Intestinal Research* **16**: 26-42.

Link, A., Balaguer, F., Shen, Y., Nagasaka, T., Lozano, J.J., Boland, C.R., Goel, A. (2010) Fecal MicroRNAs as novel biomarkers for colon cancer screening. *Cancer Epidemiology, Biomarkers & Prevention* **19**: 1766-74.

Liu, S., da Cunha, A.P., Rezende, R.M., Cialic, R., Wei, Z., Bry, L., Comstock, L.E., Gandhi, R., Weiner, H.L. (2016) The Host Shapes the Gut Microbiota via Fecal MicroRNA. *Cell Host Microbe*. **19**: 32-43.

Liu, S., Rezende, R.M., Moreira, T.G., Tankou, S.K., Cox, L.M., Wu, M., Song, A., Dhang, F.H., Wei, Z., Costamagna, G., Weiner, H.L. (2019) Oral Administration of miR-30d from Feces of MS Patients Suppresses MS-like Symptoms in Mice by Expanding Akkermansia muciniphila. *Cell Host Microbe*. **26**: 779-794.

Loddo, I., Romano, C. (2015) Inflammatory Bowel Disease: Genetics, Epigenetics, and Pathogenesis. *Frontiers in Immunology*. **6**: 551.

Macfarlane, S., Macfarlane, G.T. (2003) Regulation of short-chain fatty acid production. *Proceedings of the Nutrition Society* **62**: 67-72.

Martin, H.M., Campbell, B.J., Hart, C.A., Mpofu, C., Nayar, M., Singh, R., Englyst, H., Williams, H.F., Rhodes, J.M. (2004) Enhanced Escherichia coli adherence and invasion in Crohn's disease and colon cancer. *Gastroenterology* **127**: 80-93.

Mazmanian, S.K., Round, J.L., Kasper, D.L. (2008) A microbial symbiosis factor prevents intestinal inflammatory disease. *Nature* **453**: 620–625.

Mukhopadhya, I., Hansen, R., El-Omar, E.M., Hold, G.L. (2012) IBD-what role do Proteobacteria play? *Nature Reviews Gastroenterology & Hepatology* **9**: 219-30.

Neish, A.S. (2009) Microbes in gastrointestinal health and disease. *Gastroenterology* **136**: 65-80.

Perez-Carbonell, L., Sinicrope, F., Alberts, S., Oberg, A.L., Balaguer, F., Castells, A., Boland, C.R. & Goel, A. (2015) MiR-320e is a novel prognostic biomarker in colorectal cancer. *British Journal of Cancer* **113**, 83–90.

Phua, L.C., Chue, X.P., Koh, P.K., Cheah, P.Y., Chan, E.C., & Ho, H.K. (2014). Global fecal microRNA profiling in the identification of biomarkers for colorectal cancer screening among Asians. *Oncology Reports* **32**: 97-104.

Rashid, H., Hossain, B., Siddiqua, T., Kabir, M., Noor, Z., Ahmed, M., Haque, R. (2020) Fecal MicroRNAs as Potential Biomarkers for Screening and Diagnosis of Intestinal Diseases. *Frontiers in molecular biosciences* **7**:181.

Rawls, J.F., Mahowald, M.A., Ley, R.E., Gordon, J.I. (2006) Reciprocal gut microbiota transplants from zebrafish and mice to germ-free recipients reveal host habitat selection. *Cell* **127**: 423-433.

Round, J.L., Mazmanian, S.K. (2010) Inducible Foxp3+ regulatory T-cell development by a commensal bacterium of the intestinal microbiota. *Proceedings of the National Academy of Sciences of the United States of America* **107**: 12204–12209.

Salzman, N.H., Underwood, M.A., Bevins, C.L. (2007) Paneth cells, defensins, and the commensal microbiota: a hypothesis on intimate interplay at the intestinal mucosa. *Seminars in Immunology* **19**: 70-83.

Schönauen, K., Le, N., von Arnim, U., Schulz, C., Malfertheiner, P., Link, A. (2018) Circulating and Fecal microRNAs as Biomarkers for Inflammatory Bowel Diseases, *Inflammatory Bowel Diseases* **24:** 1547–1557.

Shi, C,. Liang, Y., Yang, J., Xia, Y., Chen, H., Han, H., Yang, Y., Wu, W., Gao, R., Qin, H. (2013) MicroRNA-21 knockout improve the survival rate in DSS induced fatal colitis through protecting against inflammation and tissue injury. *PLoS One*. **8**.

Sonnenburg, E.D., Smits, S.A., Tikhonov, M., Higginbottom, S.K., Wingreen, N.S., Sonnenburg, J.L. (2016) Diet-induced extinctions in the gut microbiota compound over generations. *Nature*. **529**: 212-215.

Teng, Y., Ren, Y., Sayed, M., Hu, X., Lei, C., Kumar, A., Hutchins, E., Mu, J., Deng, Z., Luo, C., Sundaram, K., Sriwastva, M. K., Zhang, L., Hsieh, M., Reiman, R., Haribabu, B., Yan, J., Jala, V. R., Miller, D. M., Van Keuren-Jensen, K., Merchant, M.L., McClain, C.J., Park, J.W., Egilmez, N.K., Zhang, H. G. (2018). Plant-Derived Exosomal MicroRNAs Shape the Gut Microbiota. *Cell host & microbe* **24:** 637–652.

Thursby, E., Juge, N. (2017) Introduction to the human gut microbiota. *Biochemical Journal* **474**: 1823–1836.

Turnbaugh, P. J., Hamady, M., Yatsunenko, T., Cantarel, B. L., Duncan, A., Ley, R. E., Sogin, M. L., Jones, W. J., Roe, B. A., Affourtit, J. P., Egholm, M., Henrissat, B., Heath, A. C., Knight, R., & Gordon, J. I. (2009). A core gut microbiome in obese and lean twins. *Nature* **457:** 480–484.

Ursell, L.K., Metcalf, J.L., Parfrey, L.W., Knight, R. (2012) Defining the human microbiome. *Nutrition Reviews* **70:** 38–44.

Vacca, M., Celano, G. & Calabrese, F., Portincasa, P., Gobbetti, M., De Angelis, M. (2020). The Controversial Role of Human Gut Lachnospiraceae. *Microorganisms.* **8**.

Viennois, E., Chassaing, B., Tahsin, A., Pujada, A., Wang, L., Gewirtz, A.T., Merlin, D. (2019) Host-derived fecal microRNAs can indicate gut microbiota healthiness and ability to induce inflammation. *Theranostics* **9**: 4542-4557.

Wheeler, D. A., Srinivasan, M., Egholm, M., Shen, Y., Chen, L., McGuire, A., He, W., Chen, Y. J., Makhijani, V., Roth, G. T., Gomes, X., Tartaro, K., Niazi, F., Turcotte, C. L., Irzyk, G. P., Lupski, J. R., Chinault, C., Song, X. Z., Liu, Y., Yuan, Y., Nazareth, L., Qin, X., Muzny, D.M., Margulies, M., Weinstock, G.M., Gibbs, R.A., Rothberg, J. M. (2008) The complete genome of an individual by massively parallel DNA sequencing. *Nature* **452**: 872–876.

Wohnhaas, C. T., Schmid, R., Rolser, M., Kaaru, E., Langgartner, D., Rieber, K., Strobel, B., Eisele, C., Wiech, F., Jakob, I., Gantner, F., Herichova, I., Vinisko, R., Böcher, W. O., Visvanathan, S., Shen, F., Panzenbeck, M., Raymond, E., Reber, S. O., Delić, D., Baum, P. (2020) Fecal MicroRNAs Show Promise as Noninvasive Crohn's Disease Biomarkers, *Crohn's & Colitis 360* **2.**

Yatsunenko, T., Rey, F.E., Manary, M.J., Trehan, I., Dominguez-Bello, M.G., Contreras, M., Magris, M., Hidalgo, G., Baldassano, R.N., Anokhin, A.P., Heath, A.C., Warner, B., Reeder, J., Kuczynski, J., Caporaso, J.G., Lozupone, C.A., Lauber, C., Clemente, J.C., Knights, D., Knight, R., Gordon, J.I. (2012) Human gut microbiome viewed across age and geography. *Nature* **486**: 222-227.

Zhang, L., Shen, J., Cheng, J. & Fan, X. M. (2015) MicroRNA-21 regulates intestinal epithelial tight junction permeability. *Cell Biochemistry & Function* **33:** 235-240.

Zhang, R., Xu, J., Zhao, J., Bai, J. (2017) Mir-30d suppresses cell proliferation of colon cancer cells by inhibiting cell autophagy and promoting cell apoptosis. *Tumor Biology* **39.**

6 Appendix

6.1 Zusammenfassung

Der menschliche Darm beherbergt eine komplexe Gemeinschaft von Mikroben die ständig untereinander und mit ihrem Wirt interagieren. Epitheliale Darmzellen produzieren und sezernieren miRNAs, die Zusammensetzung des Darm-Mikrobioms regulieren können. In dieser Arbeit wurde untersucht, ob und welche Mitglieder der menschlichen Darmmikrobiota synthetische miRNAs (hsa-miR-21 und hsa-miR-1226) aufnehmen können, welche in Fäkalien im Kontext einer komplexen Gemeinschaft nachgewiesen wurden (Ziel 1). Es wurde festgestellt, dass miR-1226 dazu neigt, aufgenommen zu werden und/oder mit mehreren Organismen aus der Gattung *Bacteroides* und der Gattung Ruminococcaceae (*Ruminococcus* oder *Faecalibacterium*) zu assoziieren. Weiters wurde festgestellt, dass verschiedene Gattungen der Familie Oscillospiraceae in einigen Individuen mit miR-21 assoziieren, in anderen jedoch nicht. Anschließend wurde untersucht, ob miRNAs, die einer mikrobiellen Spezies hinzugefügt wurden, deren Genexpression verändern können (Ziel 2). Es wurde beobachtet, dass das Wachstum von *B. finegoldii* und *B. thetaiotaomicron*, die in einem nährstofflimitierten Medium kultiviert wurden (aber nicht in einem reichhaltigen Medium), durch die dem Medium zugefügten miRNAs gefördert wurde. Schließlich wurden die Abundanzniveaus bestimmter fäkaler miRNAs aus Stuhlproben einer gesunden Kohorte und von Patienten mit entzündlichen Darmerkrankungen (IBD) analysiert (Ziel 3). Die wichtigsten beobachteten Unterschiede waren eine geringere Abundanz von miR-21, miR-30d und miR-320e bei IBD-Patienten im Vergleich zur gesunden Kohorte. Die hier umgesetzte Methodik und die erzielten Ergebnisse liefern wertvolle Erkenntnisse über die Wechselwirkungen zwischen fäkalen miRNAs und komplexen Darmmikrobiota-Gemeinschaften. Diese verdeutlichen den Einfluss von miRNAs auf die Zusammensetzung und Funktion der Mikrobiota in Gesundheit und Krankheit.